Seasonal variability of living benthic foraminifera from the West-Gironde mud patch (Bay of Biscay, NE Atlantic): Three contrasted periods under the stereomicroscope

C. Fontanier, B. Mamo, N. Dubosq, B. Lamarque, S. Rigaud, S. Schmidt, P. Lebleu, D. Poirier, M.-A. Cordier, A. Grémare, et al.

Seasonal variability of living benthic foraminifera from the West-Gironde Mud Patch (Bay of Biscay, NE Atlantic): Three contrasted periods under the stereomicroscope.

Fontanier* C.[1, 2, 3], Mamo B.[4], Dubosq N.[1], Lamarque B.[1], Rigaud S.[5], Schmidt S.[1], Lebleu. P.[1†], Poirier D.[1], Cordier M.-A.[1], Grémare A.[1], Deflandre B.[1]

[1]Université de Bordeaux, UMR CNRS 5805 EPOC – OASU, Allée Geoffroy Saint-Hilaire, CS 50023, F-33615 Pessac, France.

[2]FORAM, Study Group, 9 rue des Fauvettes, F-49125 Tiercé, France.

[3]Université d'Angers, 4 boulevard Lavoisier, F-49000 Angers, France.

[4]School of Natural Sciences, Macquarie University, North Ryde, NSW, 2109, Australia.

[5]Université de Nîmes, EA 7352 CHROME, rue du Dr Georges Salan, F-30021 Nîmes, France.

*Corresponding author/ Tel: +33 (0)6 21 91 93 48, c.fontanier@foram.eu.com

ORCID iD: 0000-0003-4849-6634

0. Abstract

Living continental shelf foraminifera were studied at three stations along a shore to open ocean transect between 39–69 m depth in the West-Gironde Mud Patch (WGMP) (Bay of Biscay, NE Atlantic). The aim of this work was to understand how the complex temporal variability of the environmental conditions (e.g., hydrosedimentary processes, sedimentary organic matter, oxygenation levels) controls foraminiferal ecological patterns (i.e., diversity, faunal composition, standing stock, and microhabitats). The WGMP was sampled during three different seasons (boreal summer – August 2017; winter – February 2018 and spring – April 2018), with very different meteorological patterns and benthic environmental

conditions. The sedimentary facies at the shallowest station (Station 1, 39 m) varies significantly due to hydrometeorological constraints (strong storms and swells), which are extremely marked in late autumn and during the winter. The erosion of the sandy substrate by strong bottom currents and the deposition of a silty surface layer leads to the recorded spectacular drop in foraminiferal diversity and density recorded in February and April 2018. All foraminiferal species were affected by this hydrosedimentary instability, likely due to the partial destruction of their microhabitat by intense erosional and depositional processes. At the middle WGMP station (Station 2, 47 m), benthic fauna changed much more gradually. The sedimentary imprint of the spring phytoplankton bloom is clearly recorded in April 2018 with an increase in fresh and altered phytopigment content in surface sediments. *Eggerelloides scaber*, a deposit feeder and hypoxia-tolerant species, dominated the 2017 summer foraminiferal fauna but was gradually replaced by *Ammonia falsobeccarii*, a phytophagous taxon considered quite reactive to spring bloom inputs. At the distal WGMP (Station 4, 69 m), *E. scaber* and *A. falsobeccarii* were outcompeted and gradually replaced by *Nonion faba* and *Nonionoides turgidus*, both highly adaptable species able to settle down in surface and subsurface sediments during the spring bloom periods. Able to endure a range of microhabitats and food availability, there they rely on both fresh and altered phytodetritus. We propose a conceptual scheme summarizing the putative interconnexion between foraminiferal faunas, geochemistry and physics in the WGMP.

Keywords: Benthic foraminifera; West-Gironde Mud Patch; Temporal variability; Diversity; Organic matter; Hydrosedimentary processes

1. Introduction

In the 21st century, the world's oceans are more than ever, subject to disastrous anthropogenic pressures (e.g., heavy metal and plastic pollution, overfishing) and the relentless strain imposed by uncontrollable climate change (e.g., ocean acidification, lethal marine heat waves, deoxygenation, loss of sea ice) (Halpern et al., 2015; 2019). It is vitally for us to define strategic marine areas (i.e., containing valuable resources) and to ensure their protection and sustainable management using effective environmental (bio-)indicators. It is essential to arm ourselves with the robust observation strategies to ensure rigorous and reliable environmental monitoring (e.g., Halpern et al., 2019). Within the framework of the JERICO-NEXT programme (Joint European Research Infrastructure network for Coastal Observatory-Novel European eXpertise for coastal observaTories; European Union's Horizon 2020 Research and Innovation program under grant agreement no. 654410, 2015-2019), a group of marine study areas have been defined along European coasts to exhaustively study as the ecological characteristics of benthic communities with respect to variability of physico-chemical conditions prevailing in their associated ecosystems. The major goals of this project are to assess (1) the natural interconnexion between biology, geochemistry and physics in complex shallow-water environments and (2) ascertain the quality of certain coastal areas that are currently subject or may be soon subject to anthropogenic and climate-related disturbances. Off the Gironde Estuary, the West-Gironde Mud Patch (WGMP) has been the subject of special scientific monitoring since 2009 (e.g., the BIOMIN project between 2009–2013, the VOG project between 2018–2019, the JERICO-NEXT European project with this study) (Massé et al., 2016; Lamarque et al., 2021; 2022; Dubosq et al., 2021; 2022a; Fontanier et al., 2022). This mud patch, located at a depth of 30–70 m and 40 km offshore, is important to local fisheries and a remarkable area where fine sediments accumulate and focus organic matter from an array of different sources (marine phytodetritus and continental

organic compounds) generating an area of much higher benthic diversity than would otherwise be found in such a sandy environment (Lamarque et al., 2021; 2022; Dubosq et al., 2021; 2022a; Fontanier et al., 2022). Together with the South-Gironde Mud Patch, the WGMP constitutes a particular set of morpho-sedimentary units covering the gravels and sands of the Northern Aquitaine continental shelf (Bay of Biscay, France) (Lesueur et al., 1996; 2002; Cirac et al., 2000). Both mud patches extend off the two main channels of the Gironde Estuary, the main source of the WGMP's fine-grained sediments (Fig. 1) (Lesueur et al., 1996). The WGMP comprises of Gironde River silt deposited during flood events, and a smaller portion of inner continental shelf silts and fine sand deposited during periods of high energy (i.e., storms). By combining geochemical, geophysical, sedimentological and biological analyses, the complexity of its spatial structure, temporal dynamics and environmental characteristics have been recently enlightened by a series of publications (Lamarque et al., 2021; 2022; Dubosq et al., 2021; 2022a; Fontanier et al., 2022).

Based on the extensive investigation and description of the WGMP's organic matter and sedimentary facies, Lamarque et al. (2021) demonstrated that the WGMP can be subdivided into proximal and distal areas. Each area features their own suite of surface organo-sedimentary characteristics, notably with the distal section (deeper than 42.5 m) further notably bioturbated. For this one-shot synoptic survey (i.e., a single sampling cruise performed in June 2018), there was no evidence of bottom trawling spatially impacting the WGMP, as opposed to bottom shear stress related to hydro-meteorological forcing (i.e., wind, tide, surge, and river flow). Dubosq et al. (2021) published a thorough study of the WGMP's organic carbon burial based on sedimentary facies and accumulation rates from samples collected in October 2016. Sedimentary structures indicated episodic sandy inputs overlying older deposits at proximal areas of the WGMP, and relatively continuous sedimentation in the distal area, with a maximum sediment accumulation rate (0.48 $cm.yr^{-1}$) at 47 m depth (the

depocenter of the WGMP). Organic carbon burial rates increased with water depth and reached 44 g $C.m^{-2}.yr^{-1}$ at depths greater than 62 m. Fontanier et al. (2022) have investigated the living (stained) benthic foraminifera (Eukaryota, Rhizaria, Retaria) sampled in August 2017 at 7 stations located in the WGMP. Benthic foraminifera constitute reliable proxies for studying present and past marine environments since their faunal communities (diversity, standing stock, microhabitat), spatial distribution and temporal dynamics are controlled by numerous physico-chemical parameters including exported organic matter flux, bottom- and pore-water oxygenation and sedimentary substrate (e.g., Gooday, 2003; Murray, 2006; Jorissen et al., 2007). In the WGMP, foraminiferal richness (S) presented relatively moderate values ranging between 15–35 taxa and a Shannon Index H' that distally increased with water depth. Accordingly, the relative contribution of *Eggerelloides scaber*, the dominant agglutinated species at all stations, decreased with increased depth and decreased proximity to the coast. The shallowest station (Station 1, 39 m), closest to the shore, was characterised by *E. scaber*, *Quinqueloculina laevigata* and *Ammonia beccarii*, taxa typical of inner-shelf environments constrained by high-energy hydrodynamics and river discharge. Surficial sediments at Station 1 constituted of winnowed sands depleted in organic carbon. Towards the centre of the WGMP, where clay-silt facies contained variably degraded marine phytodetritus and terrestrial organic compounds, foraminiferal faunas were characterized by *Bulimina aculeata, Ammonia falsobeccarrii, Nouria polymorphinoides* and *Nonionoides turgidus*. Yet *E. scaber* remained the most dominant taxon. Deeper stations (>55 m depth) located at the distal end of the mud patch were dominated by *B. aculeata, A. falsobeccarrii, N. polymorphinoides* and *E. scaber*. Accompanying these taxa were *Bulimina marginata, Rectuvigerina phlegeri, N. faba* and *Paracassidulina neocarinata*, which are typical of mid- and outer-shelf ecosystems enriched in sedimentary organic matter. With a temporal survey of the macrofaunal communities (4 seasonal samplings over both short [2016–2018) and long

[2010–2018) time scales), Lamarque et al. (2022) highlighted both surface sediment and benthic macrofauna spatial patterns mainly constrained by hydrodynamics. This variability reflected seasonal changes, but benthic macrofauna composition also revealed pluriannual changes corresponding to major disturbances likely caused by a series of severe storms. To summarize, previous work has shown that current hydrosedimentary processes (erosion, transport and deposition of sediments by bottom currents) substantially impact (1) the mudflat facies, (2) the distribution of sedimentary organic matter (continental vs. marine, labile vs. refractory), (3) the spatial distribution of benthic fauna (macrofauna and foraminifera) and (4) the temporal dynamics of macrofaunal communities. Interestingly, Dubosq et al. (2022a) who investigated the water column structure (temperature, salinity, dissolved, oxygen, turbidity, Chl-*a* concentration, pH) over the different seasons between 2016 and 2021, documented that a seasonal bottom water deoxygenation (oxygen saturation minimum down to 45%) occurs in late summer and autumn. This might be related to the combined effect of water column thermal stratification, the settling of organic matter produced in surface waters and the advection of deoxygenated waters from north of the Bay of Biscay.

Seasonal benthic foraminiferal variability is yet to be studied in this location and here we present a description of them during three seasons. The effect of seasonally exported phytodetritus input and the role of environmental oxygenation on benthic foraminiferal fauna has already been investigated at “La Grande Vasière”, a muddy belt located on the outer shelf (between 80–130 m deep) northwest of the WGMP (Duchemin et al., 2005; 2008) (Fig. 1). These studies have shown that living benthic fauna responds to seasonal inputs of organic matter related to phytoplankton blooms from spring to autumn. Opportunistic foraminiferal species including *Nonionella iridea* and *Cassidulina carinata* dominate the Grande Vasière mud belt fauna. This is the first reporting of seasonal benthic foraminiferal data from the WGMP, a location closer to the continental coastline than La Grande Vasière. Three stations

150 at depths between 39–69 m were sampled in August 2017 (data already published by
151 Fontanier et al. 2022), February 2018 and April 2018, covering very different periods of water
152 column structure, hydrosedimentary constraints and organic matter deposition. These three
153 stations were chosen because they have their own established faunal and environmental
154 features (Fontanier et al 2022). These include coastline-proximal modern sandy deposits at
155 one station, fine sediments at another in the depocentre part of the mud patch, and a
156 pronounced marine-influenced mudflat station at the distal part of the WGMP. To investigate
157 the seasonal changes of benthic foraminiferal fauna, we drew on geochemical, geophysical
158 and sedimentological data acquired during the 2017 and 2018 oceanographic cruises
159 JERICOBENT-2, JERICOBENT-3 and JERICOBENT-4 (Deflandre, 2017; 2018a; 2018b).
160 These data, many already published or in press (Lamarque et al., 2022; Dubosc et al., 2021;
161 2022), are compared to the faunal characteristics (diversity, standing stock, microhabitats) of
162 the sampled foraminiferal communities at the three stations to assess how complex the
163 temporal variability of the environmental conditions (e.g., organic matter, oxygenation,
164 hydrosedimentary processes) control ecological patterns. We intend to propose a conceptual
165 model depicting the putative interconnexion between the temporal dynamics of the benthic
166 fauna and the seasonal changes of the investigated ecosystems.
167

168 ## 2. Study area between August 2017 and April 2018

169 The WGMP is located between 40–80 km from the Gironde Estuary (Fig. 1). This study is set
170 up on data obtained at three stations (Stations 1, 2 and 4) sampled during the JERICOBENT-
171 2, JERICOBENT-3 and JERICOBENT-4 cruises, in August 2017, February 2018 and April
172 2018, respectively (Fig. 1; Table 1) (Deflandre, 2017; 2018a; 2018b). Sampling stations are
173 organized along a bathymetric gradient from the shallowest site and coastal (proximal) end of

174 the WGMP (Station 1, 39 m) to the deepest and most remote end (distal) of the WGMP
175 (Station 4, 69 m) (Fig. 1; Table 1).

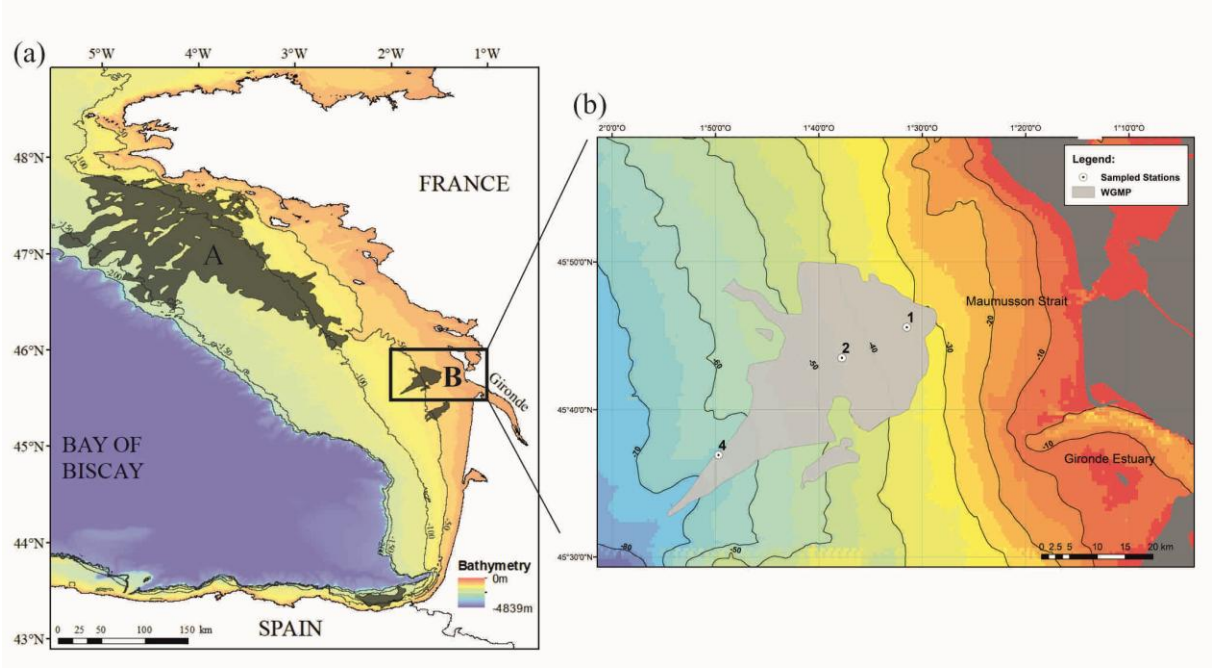

176

177 *Figure 1. (a) Map of the Bay of Biscay continental shelf with the locations of mud belts and*
178 *mud patches: A - La Grande Vasière Mud Patch pictured in dark grey and B - The West*
179 *Gironde Mud Patch pictured in dark grey (b) Map of the West Gironde Mud Patch (pictured*
180 *in light grey) showing the location of the 3 sampling stations (white dots). The synoptic map*
181 *of the WGMP has been determined during the JERICOBENT-5-TH cruise (Gillet and*
182 *Deflandre, 2018)*

183

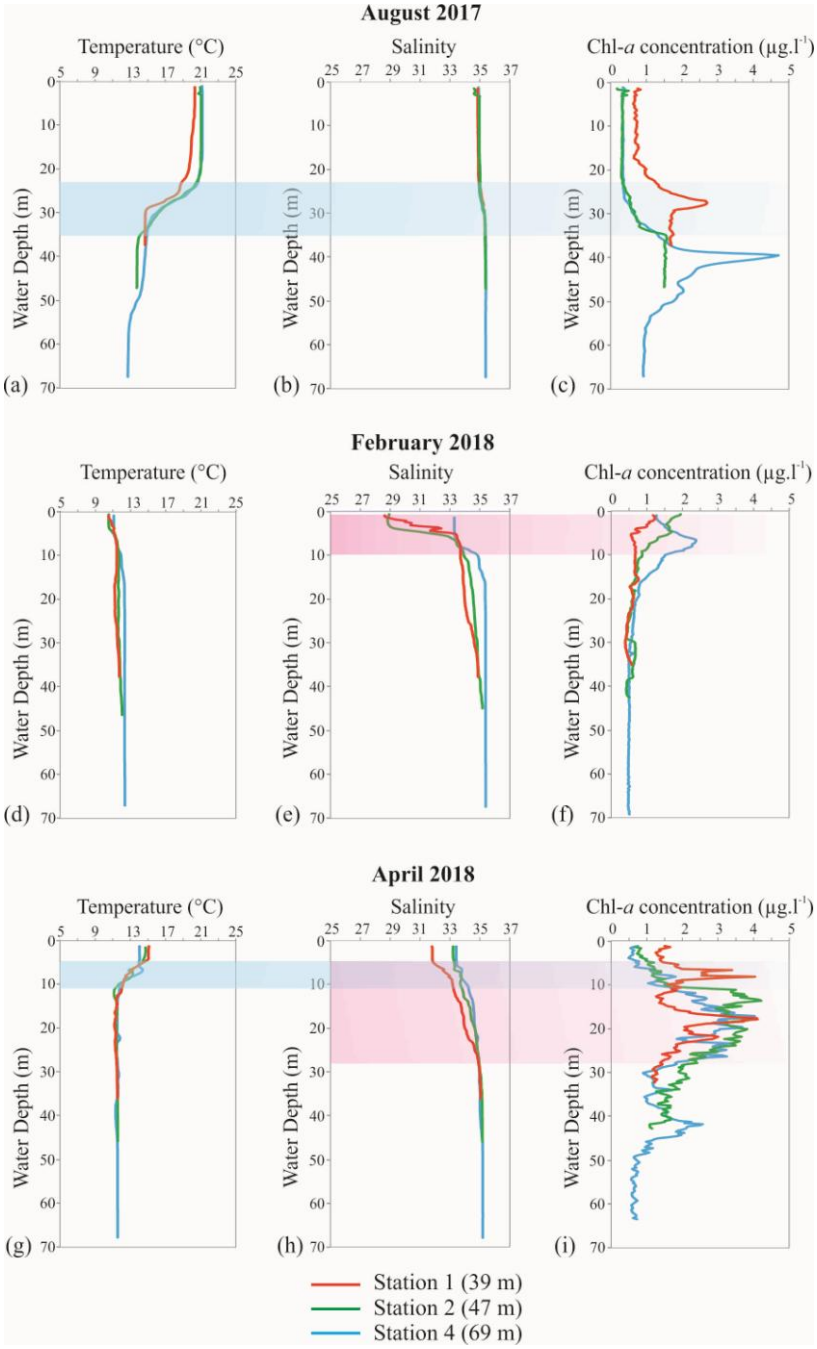

Figure 2 (a-i) CTD measurements of temperature, salinity, Chl-a concentration and turbidity in the water column at Stations 1, 2 and 4 from the WGMP (Dubosq et al., 2022a). Chl-a content is measured with CTD. The three sampling periods of August 2017, February 2018 and April 2018 are plotted. Shaded areas in blue represent mean seasonal thermoclines. Shaded areas in red represent mean seasonal haloclines. CTD Measurement data are available on SEANOE (https://www.seanoe.org/data/00783/89508/) (Dubosq et al., 2022b).

Water column temperature shows a notable seasonal change marked by (1) a strong thermocline between 20–35 m depth in August 2017 (boreal summer) (ΔT between 5–7°C depending on the station) (Fig. 2a), (2) a thermal homogenization of the water column during the following boreal winter (February 2018) (T = ~12°C) (Fig. 2d), and (3) the establishment of a new thermocline between 5–10 m depth two months later, in boreal spring (April 2018) (ΔT between 2.5–4°C depending on the station) (Fig. 2g) (Dubosq et al., 2022a; 2022b). Salinity in the water column is relatively homogeneous in August 2017 with average values close to 35, although slightly lower in the first 25 meters (Fig. 2b) (Dubosq et al., 2022a; 2022b). In February 2018, a marked halocline is recorded in the surface waters (uppermost 10 meters) with a salinity decrease toward the sea surface, that varies between stations (ΔS = 5 at Station 1, ΔS = 4 at Station 2 and ΔS = 1.5 at Station 4) (Fig. 2e). This salinity depletion is mainly related to the enhanced Gironde winter outflow and its offshore imprint (Lamarque et al., 2022; Dubosq et al., 2022a). In April 2018, a less pronounced but deeper (between 5–27 m) halocline was observable in the water column (Fig. 2h). In August 2018, chl-*a* maxima were observed in and below the summer thermocline (Dubosq et al., in press). In particular, two peaks of 2.6 $\mu g.l^{-1}$ and 4.7 $\mu g.l^{-1}$ were recorded at 28 m and 40 m depths at Station 1 and Station 4 respectively (Fig. 2c). In February 2018, moderately elevated Chl-*a* contents were mainly recorded at the sea surface at Station 1 (39 m) and to ~8 m at Station 4 (69 m) (Fig. 2e). These maxima oscillate between 1.2 $\mu g.l^{-1}$–2.4 $\mu g.l^{-1}$. At Stations 1 (depth 39 m) and 2 (47 m), near the sea floor, fluorescence tends to rise to moderate values. In April 2018, Chl-*a* values were very high in subsurface waters, especially between 5–30 m depths (at the halocline) (Fig. 2i). Numerous peaks near 4 $\mu g.l^{-1}$ were recorded at the three stations. This was the phytoplankton spring bloom already extensively described in literature (Lampert, 2001, Lampert et al., 2002; Fontanier et al., 2003). Although no water column turbidity data was available in August 2017, multi-year turbidity data shows a dramatic increase in background

water turbidity values in February 2018 at Stations 1 and 2 (65 and 50 NFU, respectively) (Dubosq et al., 2022a). This may be related to notable winter storms which occurred over the transition between 2017 and 2018 (Lamarque et al., 2022b). In April 2018, turbidity remained relatively high at Station 2 (25 NTU) but lower at Station 1 (< 9 FNU). The bottom waters of Station 4 were less turbid in all seasons (< 8 FNU) (Dubosq et al., 2022a). At each station, bottom water temperature (based on Conductivity-Temperature-Depth measurements) decreased between August 2017 and April 2018, from 14.6°C–11.6°C at Station 1 (39 m), from 13.6°C–11.6°C at Station 2 (47 m) and from 12.7°C–11.6°C at Station 4 (69 m) (Dubosq et al., 2022a) (Table 1). Bottom water salinity (Conductivity-Temperature-Depth measurements) stayed relatively constant through time and space with values ranging between 34.8–35.4 (Table 1) (Dubosq et al., 2022a). Bottom water oxygenation was high at all sites (between 184–256 µM), with the strongest values recorded in February 2018 (winter conditions) and the lowest values recorded in August 2017 (summer conditions) (Table 1) (Dubosq et al., 2022a). Oxygen penetration depth (OPD) within the sediments was relatively limited (< 0.7 cm) indicating a relatively enhanced oxygen demand to degrade organic compounds (unpublished data). Diffusive oxygen uptake (DOU) calculated according to the model by Berg et al. (1998) was at maximum at the deepest Station 4 whenever this site was sampled (Table 1) (unpublished data). Lamarque et al. (2022) have investigated the potential impact of hydro-meteorological forcings on the seafloor over our study period (Fig. 3a–b). Gironde River outflow presents a clear seasonal pattern with winter floods resulting in enhanced river discharge (e.g., 5,600 $m^3. s^{-1}$ on January the 23rd 2018) and a low-water period in summer and fall 2017 (with Gironde Estuary outflow lower than 800 $m^3. s^{-1}$). This seasonal variability has no significant impact on the spatial structuration of surface sediment characteristics in the WGMP (Lamarque et al., 2022). Bottom Shear Stress (BBS) mainly related to wind-induced swell was also calculated in Lamarque et al. (2022) (Fig. 3b).

Noticeably, the August 2017 cruise was conducted during a low-BSS episode (i.e., < 0.5 $N.m^{-2}$) as opposed to the February 2018 and the April 2018 cruises, which both took place during a high-BSS periods. Bottom Shear Stress peaks (e.g. >2.0 $N.m^{-2}$ at Station 1) in 2018 are noticeably related to late-fall and winter storms. According to Lamarque et al. (2022), high BSS values would explain the temporal changes of sediment characteristics recorded at the shallower Station 1 (39 m).

Station	Depth (m)	Latitude	Longitude	Sampling period	BWT (°C)	BWS	BWO_2 (µM)	% Sat.	OPD (cm) (N)	DOU (mmol m^{-2} d^{-1}) (N)
1	~39	45°45.550'	1°31.335'	August 2017	14.6	35.2	184.7	71.9	0.36 ± 0.16 (10)	2.87 ± 1.17 (10)
				February 2018	11.8	34.8	219.7	79.0	0.41 ± 0.08 (7)	2.82 ± 0.74 (7)
				April 2018	11.6	35.0	180.6	65.8	0.56 ± 0.29 (11)	5.76 ± 2.36 (11)
2	~47	45°43.567'	1°37.657'	August 2017	13.6	35.2	196.5	83.0	0.61 ± 0.32 (12)	3.23 ± 0.50 (12)
				February 2018	12.1	35.2	255.7	94.4	0.53 ± 0.09 (4)	4.57 ± 3.44 (4)
				April 2018	11.6	35.1	218.1	79.5	0.70 ± 0.10 (12)	4.12 ± 1.66 (12)
4	~69	45°43.993'	1°37.427'	August 2017	12.7	35.2	185.3	69.2	0.37 ± 0.08 (11)	5.92 ± 2.89 (11)
				February 2018	12.4	35.4	255.4	94.6	0.65 ± 0.08 (7)	5.53 ± 1.57 (7)
				April 2018	11.6	35.2	236.6	87.7	0.38 ± 0.06 (10)	8.96 ± 2.20 (10)

Table 1. Location of the three stations sampled during the JERICOBENT-2, -3 and -4 cruises (August 2017, February 2018 and April 2018) including station coordinates and depth. Physico-chemical parameters including BWT (bottom-water temperature in °C) and BWS (bottom-water salinity) were extrapolated from CTD casts at each site (Dubosq et al, 2022a). BWO_2 represents bottom-water oxygen in µM (Dubosq et al., 2022a). Oxygen saturation (in %) of bottom water was also calculated by Dubosq et al. (2022a). OPD (oxygen penetration depth in cm below the SWI) was determined after N in-situ measurements with a benthic profiler deployed at each station. DOU (Diffusive Oxygen Uptake in mmol m^{-2} d^{-1}) was calculated according to the model by Berg et al. (1998) (unpublished data).

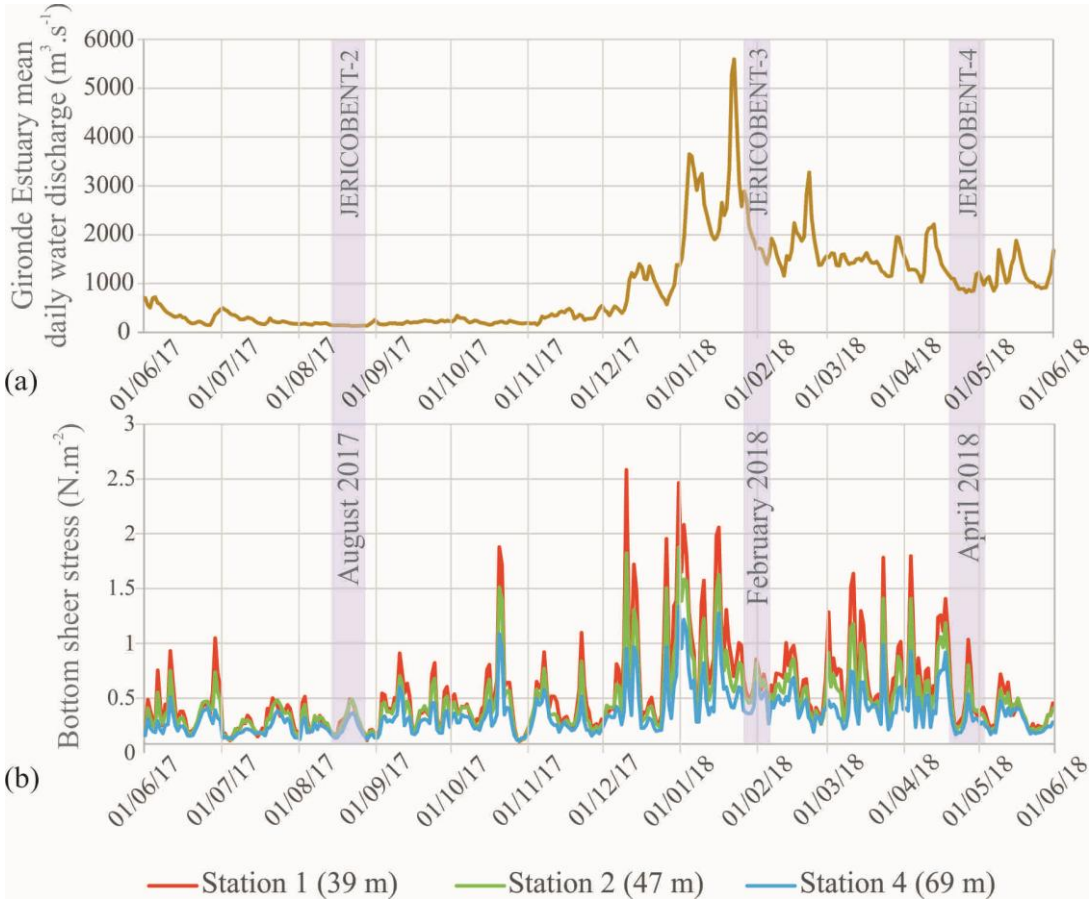

Figure 3 (a-b) Temporal changes in Gironde Estuary mean daily water discharge (a) and in the 95th percentile of Bottom Sheer Stress at stations 1, 2 and 4 (b) between June 2017 and June 2018. Sampling periods (JERICOBENT-2, -3 and -4 cruises) are indicated by shaded areas. This figure is modified from Lamarque et al. (2022) (with courtesy of B. Lamarque).

3. Material and Methods

3.1 Sediment sampling

At each station, sediment samples were gathered with a Barnett-type multiple corer equipped with Plexiglas tubes (9.6 cm internal diameter, surface area of 72 cm²) (Barnett et al., 1984). The multi-corer allowed for sampling of the uppermost decimeters of the sediment column, the overlying bottom waters, and a comparatively undisturbed sediment-water interface. At each station, the multi-corer was deployed several times (three to five) to sample enough material for geochemical, sedimentological and biological investigations. Descriptors of

sedimentary organic matter as well as the mineralization processes of organic compounds at, and below the sediment-water interface are described in detail by Dubosq et al. (2021) and Lamarque et al. (2022). We refer to a partial synthesis of their results in the discussion with data summarized in Tables 1 and 2a–b.

Station	Sampling period	OC		TN		C:N ratio		Chl-*a*	Phaeo-*a*	Chl-*a*/(Chl-*a* + Phaeo-*a*)	
		%DW	N	%DW	N		N	µg g^{-1}	µg g^{-1}		N
1	August 2017	0.31 ± 0.04	5	0.03 ± 0.00	5	12.11 ± 1.59	5	0.23 ± 0.09	1.46 ± 0.46	0.13 ± 0.02	3
	February 2018	0.28 ± 0.15	5	0.03 ± 0.01	5	10.70 ± 1.40	5	0.52 ± 0.37	2.53 ± 1.58	0.16 ± 0.02	3
	April 2018	0.92 ± 0.21	5	0.12 ± 0.03	5	9.17 ± 0.87	5	0.66 ± 0.05	3.67 ± 0.38	0.15 ± 0.01	3
2	August 2017	0.89 ± 0.06	5	0.10 ± 0.01	5	10.07 ± 1.07	5	1.15 ± 0.20	6.65 ± 0.88	0.15 ± 0.03	3
	February 2018	1.02 ± 0.54	5	0.12 ± 0.06	5	10.32 ± 1.00	5	2.09 ± 0.72	9.61 ± 2.47	0.18 ± 0.02	3
	April 2018	1.14 ± 0.39	5	0.13 ± 0.05	5	9.92 ± 0.47	5	4.54 ± 1.96	18.16 ± 8.17	0.20 ± 0.01	3
4	August 2017	1.38 ± 0.05	5	0.14 ± 0.00	5	11.16 ± 0.29	5	0.91 ± 0.18	6.90 ± 1.28	0.12 ± 0.04	3
	February 2018	1.54 ± 0.14	5	0.19+ ± 0.02	5	9.48 ± 0.57	5	1.12 ± 0.17	9.51 ± 1.86	0.11 ± 0.01	3
	April 2018	1.42 ± 0.13	5	0.18 ± 0.02	5	9.44 ± 0.48	5	5.86 ± 0.85	29.35 ± 2.83	0.17 ± 0.01	3

Station	Sampling period	$\delta^{13}C_{OM}$	$\delta^{15}N_{OM}$		THAA	EHAA	EHAA/THAA	
		‰	‰	N	mg g^{-1} DW	mg g^{-1} DW	%	N
1	August 2017	-24.44 ± 0.35	4.71 ± 0.09	2	0.51 ± 0.18	0.16 ± 0.04	32.23 ± 3.79	3
	February 2018	-25.12 ± 0.23	4.16 ± 0.27	2	0.72 ± 0.32	0.29 ± 0.12	40.97 ± 2.04	3
	April 2018	-24.29 ± 0.00	5.78 ± 0.05	2	0.98 ± 0.51	0.26 ± 0.04	29.61 ± 11.03	3
2	August 2017	-24.22 ± 0.55	5.82 ± 0.01	2	3.23 ± 0.29	0.61 ± 0.02	18.91 ± 1.36	3
	February 2018	-24.58 ± 0.48	5.80 ± 0.25	2	3.10 ± 0.16	0.59 ± 0.14	19.00 ± 4.24	3
	April 2018	-24.05 ± 0.05	5.89 ± 0.00	2	3.94 ± 0.67	0.56 ± 0.07	14.23 ± 1.44	3
4	August 2017	-24.03 ± 0.38	5.73 ± 0.12	2	4.10 ± 0.19	0.38 ± 0.02	9.14 ± 0.50	3
	February 2018	-23.91 ± 0.10	5.64 ± 0.08	2	4.32 ± 0.43	0.57 ± 0.07	13.30 ± 3.00	2
	April 2018	-23.74 ± 0.31	5.80 ± 0.14	2	4.56 ± 0.49	0.72 ± 0.20	15.27 ± 2.81	3

Table 2 Organic matter descriptors in the surface sediment (i.e. the 0–0.5 cm interval below the sediment-water interface) at the three stations sampled during the JERICOBENT-2, -3 and -4 cruises (August 2017, February, 2018 and April 2018) (Lamarque et al., 2022) : Organic content (OC in % DW), Total nitrogen content (TN in % DW), C:N atomic ratio, Chlorophyllic pigment content (i.e. Chl-a and Phaeo-a) and their freshness index Chl-a/(Chl-a+Phaeo-a), Stable carbon and nitrogen isotopic signatures of sedimentary organic matter (i.e. $\delta^{13}C_{OM}$ and $\delta^{15}N_{OM}$), Amino acid content (i.e. THAA for Totally Hydrolyzable Amino Acids and EHAA for Enzymatically Hydrolyzable Amino Acids) and their lability index (EHAA/THAA).

3.2 Sedimentological analysis

290 At each station and at the occasion of the three sampling periods, we radiographed one entire
291 core with a Scopix system, which consists of an X-Ray imaging device combined with image
292 analysis software (Migeon et al., 1999) (Fig. 4). The aim of the X-ray radiography is to detect
293 the presence of discrete sedimentary structures (e.g., coarse sedimentary layers, erosional
294 surfaces, burrows, large shells). To visually evaluate changes, we also photographed the cores
295 (Fig. 4). Particle grain size was measured with a Malvern Laser Diffraction Particle Sizer
296 (type 2600). This technique was applied to sediment samples belonging to the previously
297 radiographed and photographed core and allowed for the calculation of grain size frequency
298 D_{50}. To do so, each core was subsampled every 0.5 cm between 0–1 cm depth, every 1 cm
299 between 1–4 cm depth, then every 2 cm between 4–22 cm depth, and with an adaptative
300 resolution deeper downcore.
301
302 *3.3 Foraminiferal faunal analysis*
303 Foraminiferal fauna was examined in a single core per station. Onboard, each core was sliced
304 horizontally every 0.5 cm from the sediment-water interface to a depth of 2 cm, then every
305 centimeter between 2–10 cm depth. Samples (12 slices per core) were stored into 500 cm^3
306 bottles which were then, filled with 95% ethanol containing 2 g/L Rose Bengal stain,
307 commonly used to identify living foraminifera (Walton, 1952; Murray & Bowser, 2000).

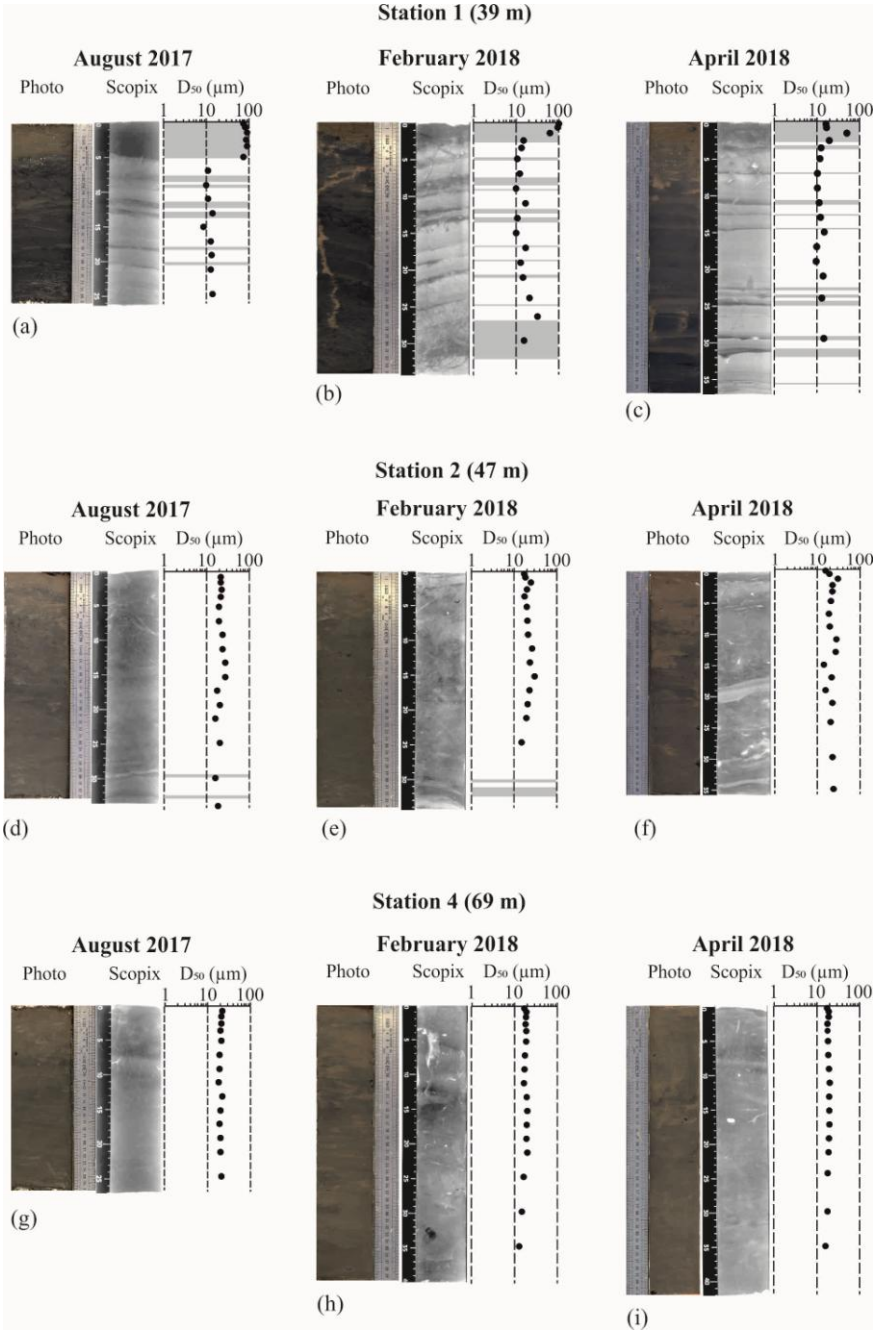

Figure 4. Photograph and X-Ray radiograph (Scopix) of split cores collected at the three stations from the WGMP with grain size frequency D_{50}. Three sampling periods (August 2017, February 2018, April 2018) are documented.

All samples were gently shaken for several minutes to obtain a homogeneous mixture. At the laboratory, samples were sieved through 150 µm mesh screens, and sieve residues were stored in 95% ethanol. Stained foraminifera belonging to the >150 µm fraction were sorted in wet

316 samples using a stereomicroscope. They were stored in Plummer slides. One concern with
317 using Rose Bengal is that it may stain the protoplasm of dead foraminifera that may be
318 relatively well-preserved for long time periods under anoxic conditions prevailing in deep
319 sediments (Corliss & Emerson, 1990; Bernhard, 2000). We therefore applied very strict
320 staining criteria (i.e., all chambers, except the last chamber, stained in bright pink), and
321 compared doubtful individuals to perfectly stained specimens of the same species found in the
322 superficial sediment layers. For miliolids, doubtful specimens were broken to inspect test
323 interior. Most stained foraminifera were identified to the species level and checked with the
324 World Foraminifera Database (Hayward et al, 2021) for current taxonomic nomenclature (see
325 Appendix A for taxonomical references and Appendix B for census data). Because samples
326 were preserved and sorted in ethanol, many soft-shelled foraminiferal species may have
327 shrunk and become unrecognizable during picking. Thus, our counts probably underestimate
328 the soft-shelled foraminiferal abundance. For each core, we calculated different indices to
329 assess diversity. First, we calculated Species Richness (S) and then Shannon index, H' (log
330 base *e*) as an information-statistic index as described in Murray (2006). We determined the
331 Berger-Parker index, which represents the highest relative contribution (%) calculated for the
332 dominant taxon at each station. Each diversity index was calculated for the entirety of each
333 core studied. Digital photographs of major species (performed with a scanning electron
334 microscope) are available in Fontanier et al. (2022).
335
336 **4. Results**
337 *4.1 Sedimentary features at the seafloor*
338 In August 2017, Station 1 was characterized by a 5 cm-thick surface layer made of very fine
339 sand (D_{50} > 75 µm) (Fig. 4a). In February 2018, a sandy surface layer was still observed (D_{50}
340 > 85 µm) but its thickness was limited to the uppermost two centimeters (Fig. 4b). In April

2018, the uppermost centimeter was characterized by clay-silt facies (D_{50} ~ 17 µm) covering a thin silty basal layer (D_{50} ~ 50 µm) (Fig. 4c). Beneath these surficial layers were dark grey sediments comprising of highly compacted and sticky mud (D_{50} ranging between 10–30 µm) within which some dense (more silty) laminae were visible (Fig. 4a-c). Regardless of sampling season, Station 2 was characterized by clay-silt facies (D_{50} ranging between 15–30 µm) throughout the sampled section (Fig. 4d–f). Horizontal, vertical and oblique biological structures (i.e., burrows) were abundant all along the cores, especially in April 2018. Station 4 presented homogeneous facies made of clayey silt (D_{50} ranging between 11–22 µm) without significant seasonal change (Fig. 4g–i).

4.2 Foraminiferal faunas (>150 µm)

4.2.1 Additional details

In this paper, we have focused on benthic foraminiferal communities above the 150 µm-size fraction as bio-indicators of environmental conditions at three different stations for three seasons (summer 2017, winter 2018 and spring 2018). Although it is recommended to study several replicates at each site to obtain a more robust, averaged view of foraminiferal faunas (Schönfeld et al., 2012), many publications on benthic foraminiferal ecology sampled in large study areas integrating various marine ecosystems do not follow this recommendation (e.g., Fontanier et al., 2002; 2022; Duchemin, 2005; 2008; Goineau et al., 2011; Dessandier et al., 2015; 2016). Environmental interpretations of modern foraminiferal faunas are frequently based on a single sample per site (eg., Fontanier et al., 2022; de Oliveira et al., 2022; Natsir, 2022; Mamo et al., 2023). We therefore consider in this study that even if small-scale (metric) spatial variability exists between benthic faunas living at the same station, this variability does not hide the faunal variability existing at the spatial scale of the WGMP, given that the three sampled stations are several kilometres apart from each other and belong to different

366 statistically derived faunal clusters (Fontanier et al. 2022). Finally, many recent studies
367 exclusively using >150 µm-sized benthic foraminifera living in the Bay of Biscay (e.g.,
368 Fontanier et al., 2002; Ersnt et al., 2005; Langezaal et al., 2006; Duchemin et al., 2005; 2008)
369 sufficiently elucidate foraminiferal diversity, standing stock and distribution on the Aquitaine
370 Shelf. Our study adds new and precious data about the temporal variability of benthic
371 environments from an inner-shelf mud patch.
372
373 *4.2.2 Standing Stocks and Diversity Indices*
374 At Station 1, total foraminiferal standing stocks decreased during the three sampling periods
375 from 4,839 individuals/100 cm² to 97 individuals/100 cm² (Fig. 5a). Accordingly, species
376 richness decreases also from 28 to 12 taxa throughout this time (Fig. 5a). The H' (/core)
377 values were low ranging between 1.59 in August 2017 and 1.84 in February 2018 (Fig. 5b).
378 Berger-Parker index (/core) decreased during the three sampling periods between 0.37–0.55.
379 At Station 2, total foraminiferal standing stocks decreased very slightly during the three
380 sampling periods between 1,835–1,690 individuals/100cm² (Fig. 5c). Species richness is
381 almost invariable (values ranging between 19 and 20 taxa). The H' (/core) increased between
382 August 2017 (1.67) and April 2018 (1.99) (Fig. 5d). Berger-Parker index (/core) decreased
383 during the three sampling periods between 0.30–0.50. At Station 3, total foraminiferal
384 standing stocks decreased during the three sampling periods between 3,319–1,706
385 individuals/100cm² (Fig. 5e). Species richness, which was higher compared to the other
386 stations, diminished between sampling seasons (values ranging between 27 and 3 taxa). The
387 H' (/core) varied between 2.26 in February 2018 and 2.38 in August 2017 (Fig. 5f). Berger-
388 Parker index (/core) increased very slightly during the three sampling periods between 0.25–
389 0.28.

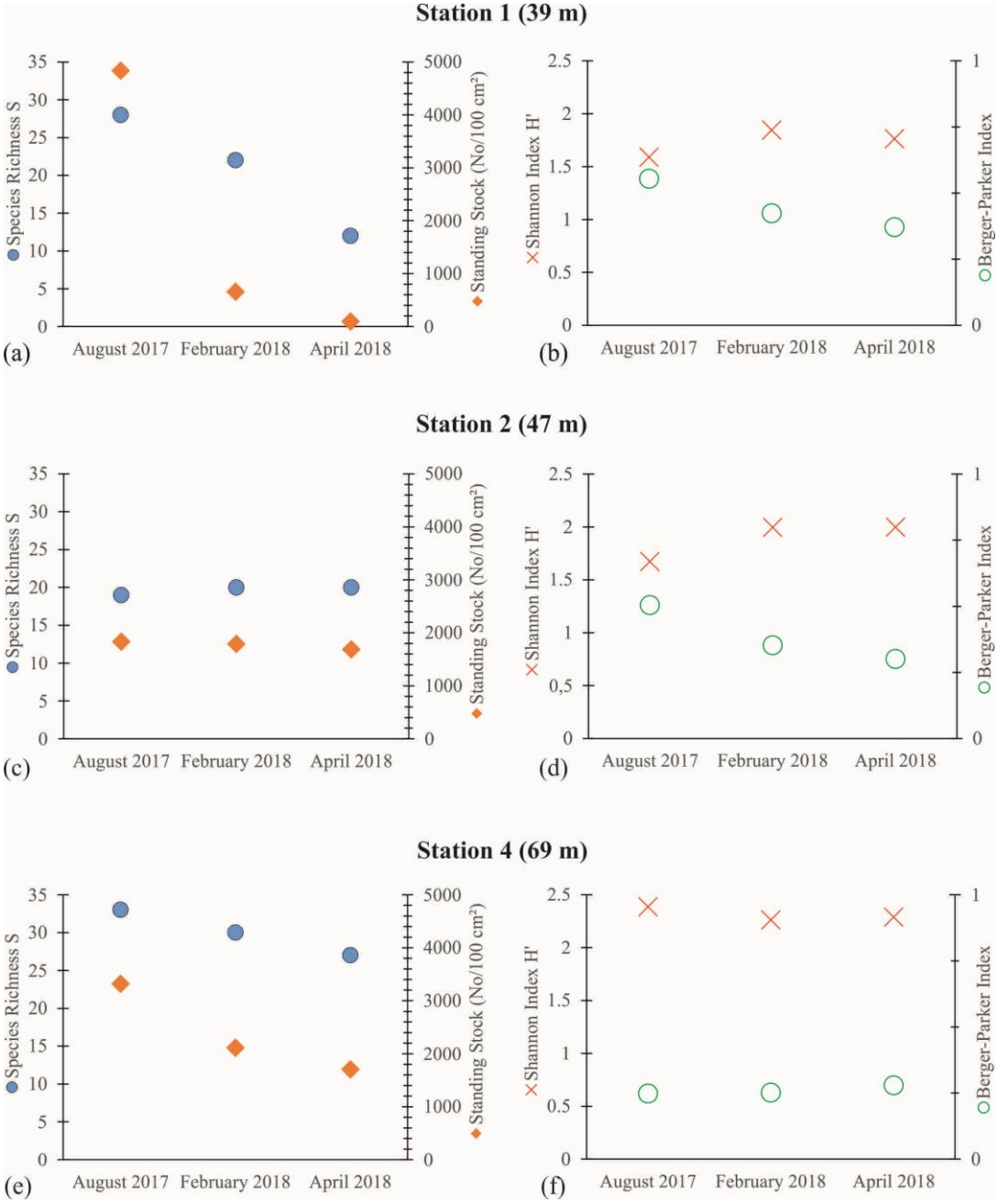

Figure 5. (a-b) Standing stockas and ecological indices describing foraminiferal faunas at the three stations 1, 2 and 4 from the WGMP during the three sampling periods. (a, c, e) Species Richness (S) and foraminiferal standing stocks (no. individuals/100 cm²); (b, d, f) Shannon (H') and Berger-Parker indices.

4.2.3 Foraminiferal Composition and Microhabitat

At Station 1, *E. scaber*, the dominant species in August 2017 (55% of the total fauna; Fig. 6a), progressively decreased in relative abundance in February and in April 2018 (42% and 27% of the total fauna, respectively; Fig. 6b–c). Its absolute density diminished noticeably from 1,931 individuals/core in August 2017 to 19 individuals/core in Spring 2018 (Appendix B). *Eggerelloides scaber* showed an erratic down-core vertical distribution with no preferential microhabitat in August 2017. Then, in February and April 2018, it thrived preferentially in the uppermost sediments with density maxima recorded in the top 3 cm (Fig. 6a). In terms of both absolute and relative abundance, *Q. laevigata* followed the same trend as *E. scaber* with values decreasing drastically between summer 2017 and spring 2018 (Fig. 6b–c and Appendix B). Its microhabitat was erratic in August 2017 and changed to a shallow infaunal preference in February and April 2018 (Fig. 6a). The relative proportion of *A. beccarii* increased from 12%–37% during the three sampling periods even if its absolute abundance decreased gradually from 423 individuals/core in August 2017 to 26 individuals/core in April 2018. Its vertical distribution also shows a preference for surficial sediments. *Bulimina aculeata* showed an increase in its relative proportion throughout the sampling period (from 6%–14%) whereas its absolute abundance decreased gradually from August 2017 to April 2018 (from 228–10 individuals/core) (Fig. 6a–c and Appendix B). It illustrated a plurimodal distribution in August 2017 and in February 2018 (Appendix B).

At Station 2, *E. scaber* (50% of the total fauna) was a dominant species during the three sampling periods but its relative contribution decreased from 50% in August 2017 to 23% in April 2018 (Fig. 6d–f). Its absolute abundance diminished from 667 individuals/core to 282 individuals/core (Appendix B). Showing an erratic down-core vertical distribution in August 2017 and in February 2018, it lived preferentially in the 0–0.5-cm interval in April 2018 (Fig. 6d–e). *Ammonia beccarii* constituted a major contributing taxon which decreased from 10%

to 5% between August 2017 and April 2018. Its absolute abundance diminished from 137 individuals/core to 68 individuals/core over the same period (Appendix B). *Ammonia beccarii* exhibited a strongly erratic down-core vertical distribution. *Bulimina aculeata* showed relative abundances ranging between 8% in February 2018 and 14% in August 2017. Its absolute abundance decreased between August 2017 and April 2018 with values ranging between 194 individuals/core and 127 individuals/core, respectively and showed a plurimodal vertical distribution. *Ammonia falsobeccarii*'s relative contribution increased over the three sampling periods (from 9% to 30% of the total fauna) (Fig. 6d–f). Its absolute abundance tripled between August 2017 and April 2018 with values ranging between 119 individuals/core and 366 individuals/core (Appendix B). *Nouria polymorphinoides* (5% of the total fauna in August 2017 increasing to 9% in April 2018) preferentially occupied the 0–0.5 cm interval in summer, then the 0.5–1 cm interval in winter and in spring 2018 (Fig. 6d–f). Its absolute abundance increased slightly between August 2017 and April 2018 with values ranging between 72 individuals/core and 111 individuals/core (Appendix B).

At Station 4, *E. scaber* was the dominant taxon in August 2017 and February 2018 (25% and 21% of the total fauna) presenting a plurimodal vertical distribution (Fig. 6g–h). Its relative abundance decreased to 7% in April 2018 (Fig.6i) and absolute abundance diminished drastically from 594 individuals/core to 90 individuals/core between August 2017 to April 2018 (Appendix B). *Ammonia falsobeccarii* relative abundance decreased gradually from 15% to 8% over the three sampling periods whereas its absolute abundance decreased from 351 individuals/core to 98 individuals/core (Fig 6g–I, Appendix B). This species preferentially occupied the uppermost centimeter of sediment. *Nonion faba* increased from 11% to 28% of the total fauna over the three sampling periods (Fig. 6g–i). Its absolute abundance increased from 256 individuals/core to 344 individuals/core between August 2017

447 and April 2018 (Appendix B). It was the most abundant between 2–4 cm in August 2017,
448 between 0.5–1.5 cm in February 2018 and between 0–1 cm in April 2018 (Appendix B).
449 *Nouria polymorphinoides,* a dominant taxon over the three sampling periods (values ranging
450 between 13% and 25% of the total fauna), preferentially occupied the uppermost 2 cm of
451 sediment. Its absolute abundance ranged between 193 individuals/core (April 2018) to 383
452 individuals/core (February 2018). *Nonionoides turgidus* was an abundant species (12%) in
453 April 2018, with 153 individuals/core (Fig. 6i, Appendix B).

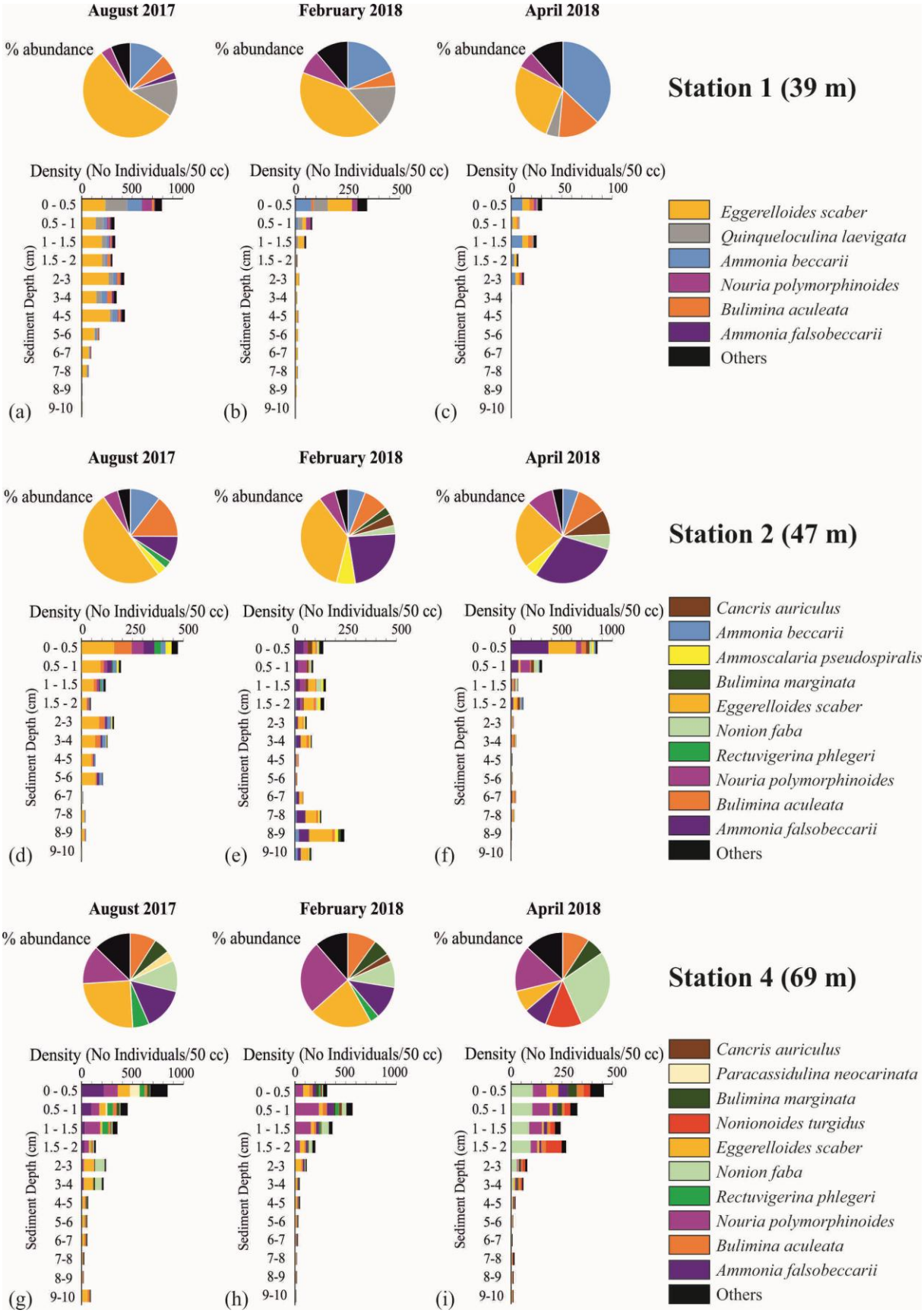

Figure 6. (a-c) Foraminiferal composition and down-core distribution of live benthic foraminifera at the three stations 1 (a), 2(b) and 4 (c) sampled in August 2017, February

2018 and April 2018. Pie charts represent the composition of live benthic foraminiferal faunas (composition in % of total fauna). The number of individuals belonging to the >150 µm-size fraction found in each level is standardized for a 50 cm^3 sediment volume. In both pie charts and core distribution, only taxa with relative abundances >2.5% are pictured.

5. Discussion

5.1. Spatial and temporal variability of the WGMP (August 2017– April 2018)

As already suggested by Lamarque et al. (2022), the comparison of our sedimentary observations with Bottom Shear Stress (BSS) data indicates that the WGMP's morphosedimentary characteristics have a seasonal variability largely dictated by hydrometeorological constraints (Fig. 3b, Fig. 4). At Station 1 (39 m), the shallowest in our transect, the sedimentary facies are the most variable. The sandy deposit observed in August 2017 was partially eroded by bottom currents likely linked to repeated storms in late autumn and the following winter, and then covered by silty surface sediments before the April 2018 sampling (Fig. 3b, Fig. 4). Water column turbidity data show the existence of a basal boundary layer a few metres thick, which was present during both February and April 2018 sampling cruises (Dubosq et al., 2022a), and which could be the product of bottom current suspension of sedimentary material at Station 1. That being said, it is always possible that this temporal variability is merely an echo of the small-scale spatial variability of the sedimentary facies at Station 1, known to be located at the boundary between the mud patch and the surrounding sandy environment (Dubosq et al., 2021). At Stations 2 (47 m) and 4 (69 m), located deeper in the mud patch, the sedimentary facies were remarkably constant over the three sampling periods. However, turbidity data also suggests the existence of a basal boundary layer at Station 2 of suspended material (Dubosq et al., 2022a). This benthic

boundary layer is present in the median zone of the WGMP and could play a fundamental role in the distribution of the finest particles and their organic load within the mud patch.

All stations show a temporal change in organic compounds accumulated below the sediment-water interface. There is a marked enrichment of fresh and altered phytodetritus (chl-*a* and phaeo-*a* content increasing over time) of a more marine origin (C:N ratio decreasing from 12 to 9) over the three seasons (Table 2). The temporal change in chlorophyll pigment content is remarkable particularly at Station 4 (from 0.9 $\mu g.g^{-1}$ to 5.9 $\mu g.g^{-1}$ for chl-*a*, from 6.9 $\mu g.g^{-1}$ to 29.3 $\mu g.g^{-1}$ for phaeo-*a*) which is also accompanied by an increase of high-lability organic matter (EHAA content increasing from 0.38 µg.g-1 to 0.72 µg.g-1 DW). Logically, diffusive oxygen uptake (DOU), which echoes the aerobic mineralization of organic compounds, is enhanced in April 2018 (Table 1). These important inputs of fresh and altered phytodetritus in the spring period are not surprising in the Bay of Biscay. They are the sedimentary expression of phytoplankton blooms occurring from the end of March until summer (e.g., Labry et al., 2001; Lampert, 2001; Lampert et al., 2002; Fontanier et al., 2003; Dubosq et al., 2022a). The warming of surface waters from the beginning of spring as well as the availability of nutrients (e.g., nitrate, phosphate) stimulates the reproduction of diatoms and coccolithophores (Lampert, 2001; González-Gil et al., 2017), resulting in high Chl-a concentration in the water column in April 2018 (Fig. 2i). But this must be considered with the contribution of the Gironde River plume and its nutrient supply to the region's surface waters as it could enhance the phytoplankton bloom in late winter and early spring (Labry et al., 2001). The sedimentary contribution of the Gironde River to the spatio-temporal dynamics of the mudflat is much more difficult to establish. The high floods recorded during the winter period, especially in January (Fig. 3a), have no effect on the C:N ratio of the organic matter of the WGMP (i.e., no increase in C:N ratio values). On the contrary, between August 2017 and February 2018 the C:N ratio of the organic compounds decreases suggesting the preferential deposition of

marine phytodetritus. Moreover, the increased remineralisation of organic compounds in spring 2018 does not seem to have a major impact on the oxygenation of the bottom water, which remains in oxic conditions (BWO_2 > 180 µmol.L^{-1}) (Dubosq et al., 2022a). This is ecologically very important considering that bottom water dysoxia (even episodic) (BWO_2 < 45 µmol.L^{-1}) can induce substantial imbalance in benthic foraminiferal communities, seasonally creating high mortality and drops in diversity (e.g., Bernhard and Sen Gupta, 1999; Murray, 2006). This does not mean that deoxygenation of the bottom waters did not occur during the autumn 2017 period (which we unfortunately did not sample). Oxygen depletion of bottom waters (between 50 and 60% of oxygen saturation) has been documented by Dubosq et al. (2022a) for the 2016 and 2021 autumnal periods. It should be noted that oxygenation is maximal at all three sites in February 2018, when winter convection allows vertical homogenisation of the water column offshore and lateral advection of well-oxygenated water along the shelf floor (González-Gil et al., 2017). In figure 7, we propose a conceptual scheme showing the summarised impact of hydrometeorological conditions (storms and associated high swells) as well as the importance of the phytoplankton bloom on the sediment structuring of the WGMP (inorganic sediments and organic matter) between August 2017 and April 2018.

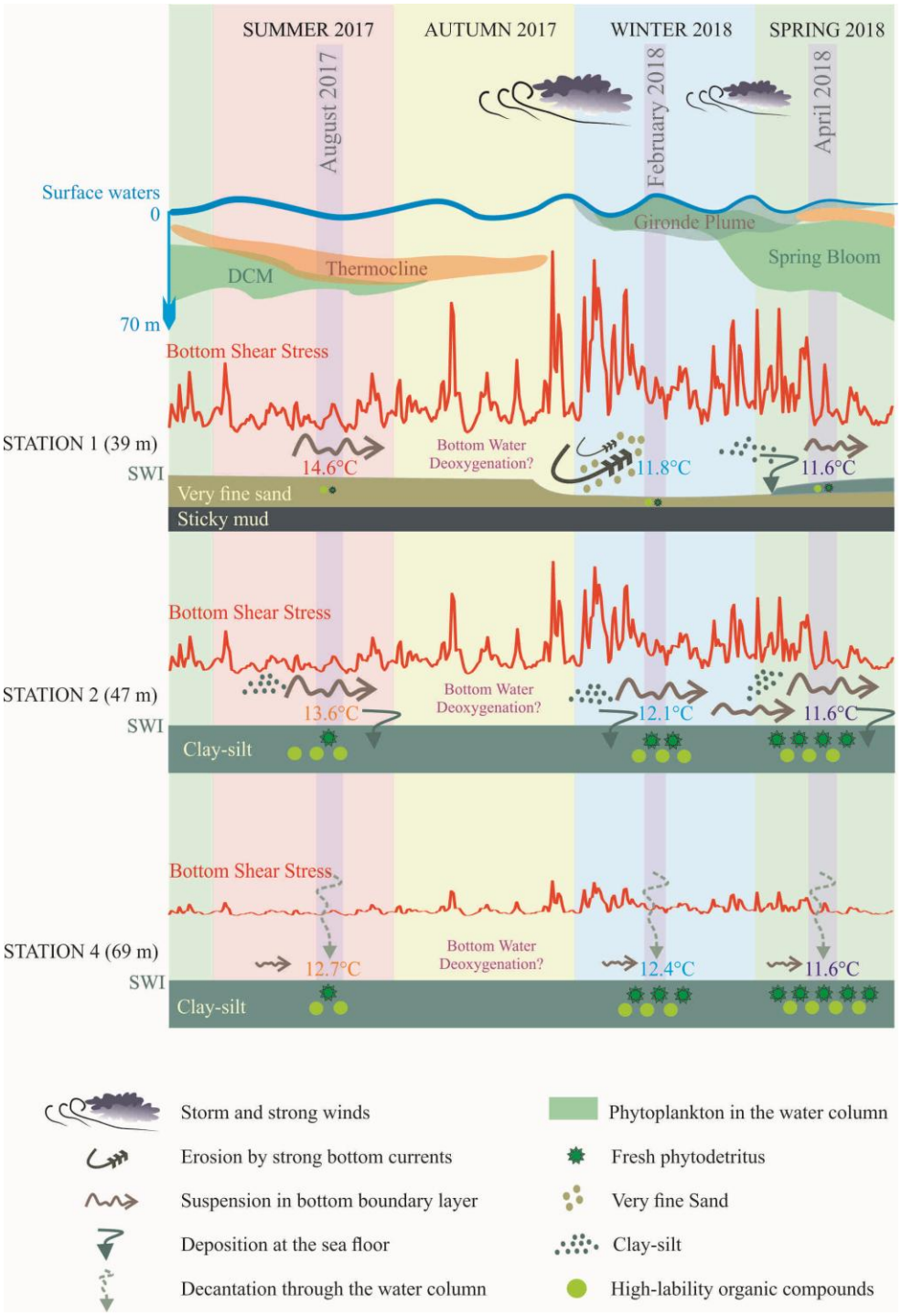

Figure 7. Conceptual diagram representing the spatial and temporal variability of the West-Gironde Mud Patch between summer 2017 and spring 2018. The hydrosedimentary processes (e.g., erosion, suspension) presumed to impact the sediment-water interface (SWI) of the three stations (Station 1, 2 and 4) are pictured by signs explained in the legend. The major hydrometerological conditions retained in this figure vary depending on the depth of the

sample site and are expressed via BSS values (Lamarque et al., 2021). Both the Gironde River plume, which is clearly documented in winter, and spring phytoplankton bloom are pictured. Bottom Water Temperatures (BWT) and the approximate position of the thermocline in the water column are exhibited along with sedimentary features and concentration of sedimentary organic compounds (fresh phytodetritus, labile compounds). A Deep Chlorophyll Maximum (DCM) is illustrated during the summer stratification of surface waters.

5.2 Benthic foraminiferal variability

5.2.1 The proximal mud patch – Station 1

The most remarkable feature of our living benthic foraminiferal dataset is the impressive drop in faunal diversity and standing stocks at Station 1 between August 2017 and April 2018 (S decreasing from 28 to 12 taxa and standing stocks decreasing from 4,839 individuals/100 cm² to 97 individuals/100 cm²) (Fig. 5a, Fig. 6a–c, Fig. 8). Such an alteration of the unicellular meiofauna cannot be the result of any autumnal bottom-water deoxygenation. Foraminiferal fauna can undergo compositional change, a drop in abundance and decreased diversity when bottom water oxygenation reaches critical values (i.e., dysoxia, <45 µmol.L^{-1}) (Bernard and Sen Gupta, 1999), but this is not the case in our study area, where bottom water stays oxic even during so-called deoxygenation events (Dubosq et al., 2022a). It seems simplistic, to hold a drop in bottom water temperature (by 3°C) as solely responsible for this faunal decline (Gross, 2000). *Eggerelloides scaber*, the dominant species of Station 1, can live and dominate benthic faunas in the colder waters of the North Sea Shelf (see literature review by Murray, 2006). The cause of this faunal regression must be sought in the impact of hydrosedimentary conditions on the microhabitats occupied by foraminifera. The erosive and depositional processes hypothesised to have impacted Station 1 during the winter (Fig. 7) may constitute extremely restrictive ecological parameters for benthic fauna. In submarine canyons subject to

554 turbidity flows or on continental shelves subject to the colossal energy of a tsunami, benthic
555 faunas with low diversity are documented (Hess et al. 2005; Tsujimoto et al, 2020). Faunal
556 communities reflect the remnants of moribund adult assemblage or the first stages of a
557 recolonising substrate following the physical disturbance that destroyed the original benthic
558 habitat (e.g., Anchutz et al., 2002; Hess et al., 2005; Koho et al., 2007; Hess and Jorissen,
559 2009; Toyofuku et al., 2014). Opportunistic pioneer species can then be observed in low-
560 diversity faunas (such as *Psammosphaera fusca* in Toyofuku et al., 2014). The same applies
561 to ecosystems in prodeltaic zones subject to sedimentary instability often linked to the inflow
562 of coastal rivers (Goineau et al., 2012). In these situations, benthic fauna can be reduced to a
563 single species, as illustrated by the over-dominance of *Leptohalysis scottii* in a 24 m-depth
564 station located 2 km from the mouth of the Rhône prodelta (Goineau et al., 2012). The
565 appearance of this opportunistic pioneer taxon followed an exceptional flood of the Rhône
566 and the sudden deposition of massive muddy sediments. In our case, the faunal composition
567 of Station 1 changed very little between August 2017 and April 2018 (Fig. 8). *Eggerelloides*
568 *scaber*, *A. beccarii* and *Quinqueloculina* spp. which are dominant at all 3 sampling periods,
569 are usually considered as neritic species living in shallow benthic environments with high
570 hydrodynamic energy and often connected to river mouths (e.g., Barmawidjaja et al, 1992;
571 Debenay and Redois, 1997; Diz et al, 2006; Diz and Francés, 2008; Goineau et al, 2011;
572 2012; Mendes et al, 2012; Dessandier et al, 2015; 2016; Fontanier et al, 2022). These taxa
573 seem to struggle within the proximal mud patch due to the probable partial destruction of their
574 microhabitat by intense erosional and depositional processes.

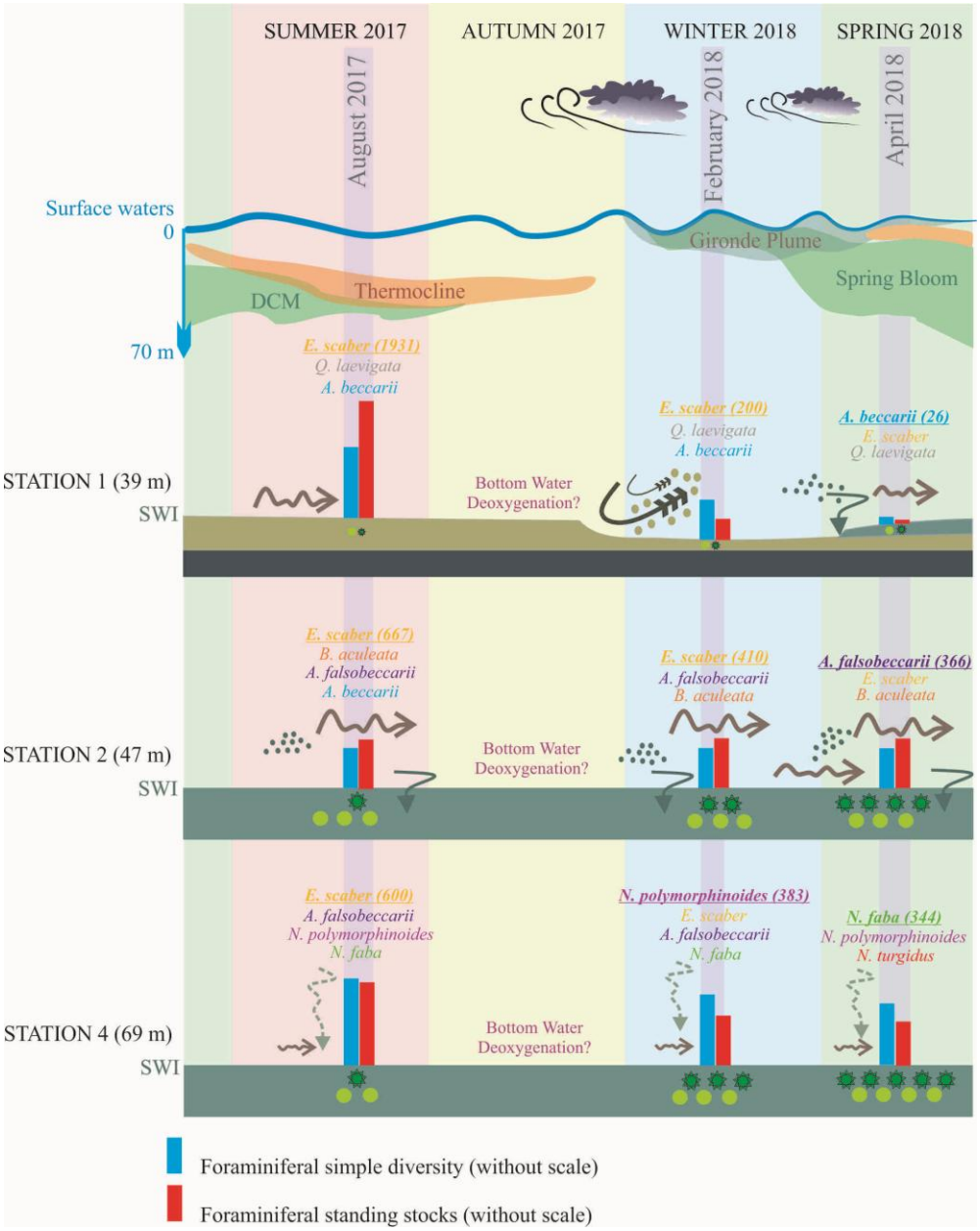

575

576 *Figure 8. Conceptual diagram representing the spatial and temporal variability of*
577 *foraminiferal faunas (>150 µm size fraction) in the West-Gironde Mud Patch between*
578 *summer 2017 and spring 2018. The hydrosedimentary processes (e.g., erosion, suspension,*
579 *deposition) assumedly affecting the water-sediment interface (SWI) of the three stations*
580 *(Station 1, 2 and 4) are represented by figures explained in Figure 8. The nature of the*
581 *sediments and the concentration of different sedimentary organic compounds are also shown*
582 *(see caption of Figure 8 for further information). Underlined species are dominant in terms of*
583 *relative abundance. The values between parentheses indicate the number of individuals per*

core. The blue bars represent the simple diversity S. The red bars indicate the total foraminiferal standing stocks. The height of the bars is used for comparison.

5.2.2 The median mud patch – Station 2

Although *E. scaber* is the dominant species at Station 2 in August 2017 and February 2018, its absolute and relative abundances decrease over the three sampling periods. Absolute abundance was diminished from 667 individuals/core to 282 individuals/core, and relative abundance was decreased from 50% in August 2017 to 23% in April 2018 (Fig. 6d–f, Fig. 8). In contrast, *A. falsobeccarii*, which is also a major species within the mud patch, shows a gradual increase of absolute and relative abundances between summer 2017 and spring 2018 (threefold increase in standing stocks) (Fig. 6d-f, Fig. 8). This pattern follows the progressive enrichment of surface sediments in fresh and degraded phytopigments as well as the relative increase in OC content (Table 2, Fig. 7). This faunal trend suggests that phytodetritus plays a significant ecological role in the seasonal dynamics of *A. falsobeccarii*, making a phytophagous taxon quite reactive to the spring bloom inputs. This is unlike *E. scaber*, which is more adapted to rely on altered and deeply buried organic compounds (Fontanier et al., 2022). The erratic vertical distribution of *E. scaber* within anoxic sediments at our three stations (Fig. 6a–i) underlines its capacity to thrive under low oxygenation without any preference for fresh food (Diz et al., 2006; Langlet et al., 2014). Such behavior has also been documented in laboratory experiments simulating hypoxia and/or organic supply with sediment material sampled in the Bay of Biscay (Ernst et al., 2005). The microhabitat of *A. falsobecarrii,* restricted to the first half centimetre below the sediment-water interface in April 2018 (Fig. 6f) seems to argue for its trophic preference for freshly deposited phytodetritus. However, it is of note that this assumed seasonal response of *A. falsobeccarii* does not result in a general increase in the standing stock of benthic foraminiferal fauna, as might be

609 expected when opportunistic species react strongly to changes in preferred food supply. Only
610 some other secondary species (*Nouria polymorphinoides, Cancris auriculus, N. faba*) show a
611 notable but moderate burst of their absolute abundance in spring 2018. This could be linked to
612 the fraction studied in this paper (>150 µm size fraction) which does not necessarily include
613 the most opportunistic taxa, those of small size such as *Epistominella* spp., *Bolivina* spp. and
614 *Cassidulina* spp. which can develop significant numbers in a few weeks after a sudden influx
615 of phytodetritus (e.g., Fontanier et al., 2003; Duijnstee et al., 2004; Langezaal et al., 2006;
616 Duchemin et al., 2008; Goineau et al., 2012).
617
618 *4.2.3 The distal mud patch – Station 4*
619 At Station 4, the empirical relationship linking *A. falsobeccarii* to the seasonal enrichment of
620 surface sediments in chlorophyll pigment is not reflected. On the contrary, its relative and
621 absolute abundances decrease over the three sampling periods while the sediment is gradually
622 enriched in fresh and degraded chlorophyll-a (relative abundance decreasing gradually from
623 15% to 8% over the three sampling periods, absolute abundance decreasing from 351
624 individuals/core to 98 individuals/core) (Fig. 6g–i, Fig. 8). The apparent interpretive
625 contradiction between the observations made at Stations 2 and 4 could be explained by the
626 role of biotic factors on the development of the different foraminiferal populations. The
627 regression of *A. falsobeccarii* (and also *E. scaber*) could be linked to the competition between
628 species for access to different food sources. This interspecific constraint is often neglected in
629 the understanding of the ecology of benthic foraminifera. At Station 4, the most
630 taxonomically diverse of the stations studied, *N. faba* and *N. turgidus* are better adapted than
631 *A. falsobeccarii* to take advantage of seasonal inputs of fresh and degraded phytodetritus.
632 Their respective ability to occupy deeper microhabitats in the sediment allows them to access
633 more degraded organic matter buried deep in the sediment, especially in spring 2018 (Fig. 6i).

In fact, *N. faba* is commonly described in mid- and outer-shelf environments including from subsurface sediments (e.g., Debenay and Redois, 1997; Fontanier et al., 2002; Langezaal et al., 2006; Duchemin.et al., 2005; 2008; Goineau et al., 2011; Dessandier et al., 2015; 2016). This species dominates the >150 µm-sized faunas sampled between 80–140 m depth in La Grande Vasière mud belt in the Bay of Biscay (NE Atlantic), especially in spring during the bloom period (Duchemin et al., 2005; 2008). Documented as a deep infaunal dweller at a 150 m-depth station in the Southern Bay of Biscay (Langezaal et al., 2006), this taxon is capable of migration upward to surface sediments to access fresher phytodetritus . This microhabitat and trophic plasticity makes *N. faba* an excellent competitor for space and food during spring bloom episodes in the WGMP. *Nonionoides turgidus* is a very reactive species within the distal part of the mud patch (its standing stocks increasing from 11 individuals/core in February to 153 individuals/core in April). Goineau et al. (2011) also documented the dominance of *N. turgidus* (*Nonionella turgida* in their study) at depths ranging between 47–62 m close to the Rhône River mouth. There, this species takes advantage of terrestrial and marine organic compounds buried within the sediments (Goineau et al., 2011; 2012). *N. turgidus* has been documented in the La Grande Vasière mud belt where it dominates autumnal faunas to benefits from the combination of continental organic matter and altered marine phytodetritus (Duchemin et al., 2008).

6. Conclusions

Living shelf foraminiferal faunas have been studied at three stations located along a shore to open ocean transect between 39–69 m depth in the West-Gironde Mud Patch (WGMP) (Bay of Biscay, NE Atlantic) to understand how complex the temporal variability of the environmental conditions (e.g., hydrosedimentary process, sedimentary organic matter, oxygenation level) control their ecological patterns (i.e., diversity, faunal composition,

659 standing stock, and microhabitats). To do so, the WGMP was sampled in August 2017 (boreal
660 summer), February 2018 (winter) and April 2018 (spring), which are very different in terms
661 of meteorological patterns and benthic environmental conditions. The main findings of this
662 study are:
663
664 (1) The shallowest station (Station 1, 39 m) closest to shore is subject to significant
665 variability in sedimentary facies in relation to hydrometeorological constraints (strong
666 storms and swells), which are extremely marked in late autumn and throughout winter.
667 The erosion of the sandy substrate by strong bottom currents and the deposition of
668 silty surface layer leads to a marked drop in the diversity and density of adult
669 foraminifera in February and April 2018. All species are affected by this
670 hydrosedimentary instability, due to the partial destruction of their microhabitat by
671 intense erosional and depositional processes.
672 (2) At the station located in the central area of the WGMP (Station 2, 47 m), benthic fauna
673 changes in a more gradual manner. The sedimentary imprint of the spring
674 phytoplankton bloom is clearly recorded in April 2018 with an increase in fresh an
675 altered phytopigment content in the surface sediment. *Eggerelloides scaber*, a deposit
676 feeder and hypoxia-tolerant species, dominated the 2017 summer foraminiferal fauna
677 and was gradually replaced by *A. falsobeccarii* which may be considered a
678 phytophagous taxon that is reactive to spring bloom inputs.
679 (3) At the most ocean-ward station of the WGMP (Station 4, 69 m), *E. scaber* and *A.*
680 *falsobeccarii* are outcompeted and gradually replaced by *N. faba* and *N. turgidus.*
681 Both species present microhabitat and dietary plasticity that helps them to settle in
682 surface and subsurface sediments during the spring bloom period. There, they rely on
683 both fresh and altered phytodetritus.

Acknowledgement

We would like to thank the crews and the captain of the Côte de la Manche (CNRS-INSU) during the JERICOBENT-2, JERICOBENT-3 and JERICOBENT-4 cruises. We have special thoughts for all scientific members who participated to this scientific mission. This work was supported by: (1) the JERICO-NEXT project (European Union's Horizon 2020 Research and Innovation program under grant agreement no. 654410), (2) the VOG project (LEFE-CYBER and EC2CO-PNEC), and (3) the MAGMA project (COTE cluster of Excellence ANR-10-LABX-45). Finally, we thank all reviewers who have provided very useful comments to improve the overall quality of this paper.

References

Barmawidjaja, D.M., Jorissen, F.J., Puskaric, S. and Van Der Zwaan, G.J., 1992. Microhabitat selection by benthic foraminifera in the northern Adriatic Sea. Journal of Foraminiferal Research. 22(4), 297-317.

Anschutz, P., Jorissen, F.J., Chaillou, G., Abu-Zied, R. and Fontanier, C., 2002. Recent turbidite deposition in the eastern Atlantic: Early diagenesis and biotic recovery. Journal of Marine Research, 60, 835-854.

Barnett, P.R.O., Watson, J. and Connely, D., 1984. A multiple corer for taking virtually undisturbed sample from shelf, bathyal and abyssal sediments. Oceanologica Acta, 7, 399-408.

Berg, P., Risgaard-Petersen, N. and Rysgaard, S., 1998. Interpretation of measured concentration profiles in sediment pore water. Limnology and Oceanography, 43, 1500-1510.

Bernhard, J.M. and Sen Gupta, B.K., 1999. Foraminifera in Oxygen-Depleted Environments. In: Sen Gupta, B.K., Ed., Modern Foraminifera, Kluwer, Dordrecht, 201-216.

Bernhard, J.M., 2000. Distinguishing live from dead foraminifera: Methods review and proper applications. Micropaleontology, 46(1), 38-46.

Berthois, L. and Le Calvez, Y., 1959. Deuxième contribution à l'étude de la sédimentation dans le golfe de Gascogne. Revue des Travaux de l'Institut des Pêches Maritimes, vol. 23 n° 3: 323-375.

Cirac, P., Berné, S., Castaing, P. and Weber, O., 2000. Processus de mise en place et d'évolution de la couverture sédimentaire superficielle de la plate-forme nord-aquitaine. Oceanologica Acta, 23/6, 663-686.

Corliss, B.H. and Emerson, S., 1990. Distribution of Rose Bengal stained deep-sea benthic foraminifera from the Nova Scotia continental margin and Gulf of Maine. Deep-sea Research, 37, 381-400.

Cushman, J.A., 1931. The Foraminifera of the Atlantic Ocean. Part 8. Rotaliidae, Amphisteginidae, Calcarinidae, Cymbaloporettidae, Globorotaliidae, Anomalinidae, Planorbulinidae, Rupertiidae and Homotremidae. Bull. U.S. Natl. Mus. 104.

de Oliveira, T. R. S., dos Santos, L. D., Eichler, P. P. B., Barker, C. P. and Barcellos, R. L., 2022. Benthic Foraminifera of Tropical Estuarine-Lagoonal-Bays System, in the Suape Harbor, Brazil: A Case Study. Journal of Foraminiferal Research, 52(1), 4-20. doi: 10.2113/gsjfr.52.1.4

Debenay, J.P. and Redois, F., 1997. Distribution of the twenty seven dominant species of shelf benthic foraminifers on the continental shelf, north of Dakar (Senegal). Marine Micropaleontology, 29(3-4), 237-255.

Deflandre, B., 2016. JERICOBENT-1 cruise, Côtes De La Manche R/V. https://doi.org/10.17600/16010400

733 Deflandre, B., 2017. JERICOBENT-2 cruise, Côtes De La Manche R/V.
734 https://doi.org/10.17600/17011000
735 Deflandre, B., 2018a. JERICOBENT-3 cruise, Côtes De La Manche R/V,
736 https://doi.org/10.17600/18000469
737 Deflandre, B., 2018b. JERICOBENT-4 cruise, Côtes De La Manche R/V,
738 https://doi.org/10.17600/18000470
739 Dessandier, P.-A., Bonnin, J., Kim J.-H., Bichon, S., Grémare, A., Deflandre, B., de Stigter,
740 H. and Malaizé, B., 2015. Lateral and vertical distributions of living benthic
741 foraminifera off the Douro River (western Iberian margin): Impact of the organic
742 matter quality. Marine Micropaleontology, 120, 31–45.
743 Dessandier, P.-A., Bonnin, J., Kim J.-H., Bichon, S., Deflandre, B., Grémare, A. and
744 Sinninghe Damsté, J. S., 2016. Impact of organic matter source and quality on living
745 benthic foraminiferal distribution on a river-dominated continental margin: A study of
746 the Portuguese margin. Journal of Geophysical Research: Biogeosciences, 121, 1689–
747 1714. https://doi.org/10.1002/2015JG003231.
748 Diz, P., Francés, G. and Roson, G., 2006. Effects of contrasting upwelling-downwelling on
749 benthic foraminiferal distribution in the Ria de Vigo (NW Spain). Journal of Marine
750 Systems, 60, 1-18.
751 Diz, P. and Francés, G., 2008. Distribution of live benthic foraminifera in the Ría de Vigo
752 (NW Spain). Marine Micropaleontology, 66(3-4), 165-191.
753 Dubosq, N, Schmidt, S, Walsh, J. P., Grémare, A., Gilet, H., Lebleu, P., Poirier, D, Perello,
754 M.-C., Lamarque, B. and Deflandre, B., 2021. A first assessment of organic carbon
755 burial in the West Gironde Mud Patch (Bay of Biscay). Continental Shelf Research.
756 221, 104419 (11p.). https://doi.org/10.1016/j.csr.2021.104419.

Dubosq, N., Schmidt, S., Sudre, J., Rigaud, S., Lamarque, B., Danilo, M., Grémare, A. and B. Deflandre, 2022a. First observations of seasonal bottom water deoxygenation off the Gironde estuary (Bay of Biscay, North East Atlantic). Frontiers in Marine Science, 9, https://doi.org/10.3389/fmars.2022.1006453

Dubosq, N., Schmidt, S. and Deflandre, B., 2022b. Vertical distributions of temperature, salinity, dissolved oxygen concentrations and saturations, Chl-a, turbidity and pH in the water column of the continental shelf off the Gironde (North East Atlantic, France). SEANOE. https://doi.org/10.17882/89508

Duchemin, G., Jorissen, F.J., Andrieux-Loyer, F., Le Loc'h, F., Hily, C. and Philippon, X., 2005. Living benthic foraminifera from "La Grande Vasière", French Atlantic continental shelf: faunal composition and microhabitats. Journal of Foraminiferal Research, 35, 198-218.

Duchemin, G., Jorissen, F.J., Le Loc'h, F., Andrieux-Loyer, F., Hily, C. and Thouzeau, G., 2008. Seasonal variability of living benthic foraminifera from the outer continental shelf of the Bay of Biscay. Journal of Sea Research, 59(4), 297-319.

Duijnstee, I., de Lugt, I., Vonk Noordegraaf, H. and van der Zwaan, B., 2003. Temporal variability of foraminiferal densities in the northern Adriatic Sea. Marine Micropalontology, 50, 125-148.

Ernst, S., Duijnstee, I., Fontanier, C., Jorissen, F.J. and Van der Zwaan, B., 2005. A comparison of foraminiferal infaunal distributions in field and experimental samples from 550-m depth in the Bay of Biscay. Deep Sea Research Part I: Oceanographic Research Papers, 55 (4), 498-518

Fontanier, C., Jorissen, F.J., Licari, L., Alexandre, A., Anschutz, P. and Carbonal, P., 2002. Live benthic foraminiferal faunas from the Bay of Biscay: faunal density,

781 composition, and microhabitats. Deep Sea Research Part I: Oceanographic Research
782 Papers, 49(4), 751-785.
783 Fontanier, C., Jorissen, F.J., Chaillou, G., David, C., Anschutz, P. and Lafon, V., 2003.
784 Seasonal and interannual variability of benthic foraminiferal faunas at 550 m depth in
785 the Bay of Biscay. Deep Sea Research Part I: Oceanographic Research Papers, 50(4),
786 457-494.
787 Fontanier, C., Deflandre, B., Rigaud, S., Mamo, B., Dubosq, N., Lamarque, B., Langlet, D.,
788 Schmidt, S., Lebleu, P., Poirier, D., Cordier, M.-A. and Grémare, A., 2022. Live
789 (stained) benthic foraminifera from the West-Gironde Mud Patch (Bay of Biscay, NE
790 Atlantic): Assessing the reliability of bio-indicators in a complex shelf sedimentary
791 unit. Continental Shelf Research. 232, 104616 (13p.).
792 https://doi.org/10.1016/j.csr.2021.104616
793 Gillet, H. and Deflandre, B., 2018. JERICOBENT-5-TH cruise, Thalia R/V.
794 https://doi.org/10.17600/18000425
795 Glud, R.N., Gundersen, J.K., Jorgensen, B.B., Revsbech, N.P. and Schulz, H.D., 1994.
796 Diffusive and total oxygen uptake of deep-sea sediments in the eastern South Atlantic
797 Ocean: In situ and laboratory measurements. Deep-Sea Research Part I:
798 Oceanographic Research Papers. 41(11 /12), 1767-1788.
799 Goineau, A., Fontanier, C., Jorissen, F.J., Lansard, B., Buscail, R., Mouret, A., Kerhervé, P.,
800 Zaragosi, S., Ernoult, E. and Artéro, C., 2011. Live (stained) benthic foraminifera
801 from the Rhône prodelta (Gulf of Lion, NW Mediterranean): Environmental controls
802 on a river-dominated shelf. Journal of Sea Research, 65, 58–75.
803 Goineau, A., Fontanier, C., Jorissen, F., Buscail, R., Kerhervé, P., Cathalot, C., Pruski, A.M.,
804 Lantoine, F., Bourgeois, S. and Metzger, E., 2012. Temporal variability of live
805 (stained) benthic foraminiferal faunas in a river-dominated shelf – Faunal response to

806 rapid changes of the river influence (Rhône prodelta, NW Mediterranean).
807 Biogeosciences, European Geosciences Union, 9 (4), 1367-1388.
808 González-Gil, R., González Taboada, F., Cáceres, C., Largier, J. L. and Anadón, R., 2017.
809 Winter-mixing preconditioning of the spring phytoplankton bloom in the Bay of
810 Biscay. Limnology and Oceanography, 63, 1264-1282.
811 Gooday, A.J., 2003. Benthic Foraminifera (Protista) as tools in Deep-water
812 Palaeoceanography: Environmental Influences on Faunal Characteristics. Advances in
813 Marine Biology, 46, 1-90.
814 Gross, O., 2000. Influence of temperature, oxygen and food availability on the migrational
815 activity of bathyal benthic foraminifera: evidence by microcosm experiments. In:
816 Liebezeit, G., Dittmann, S., Kröncke, I. (eds) Life at Interfaces and Under Extreme
817 Conditions. Developments in Hydrobiology, vol 151. Springer, Dordrecht.
818 https://doi.org/10.1007/978-94-011-4148-2_12
819 Halpern, B. S., Frazier, M., Potapenko, J., Casey, K. S., Koenig, K., Longo, C., Lowndes, J.
820 S., Rockwood, R. C., Selig, E. R., Selkoe, K. A. and Walbridge, S., 2015. Spatial and
821 temporal changes in cumulative human impacts on the world's ocean. Nature
822 Communications, 6, 7615.
823 Halpern, B. S., Frazier, M., Afflerbach, J., Lowndes, J. S., Micheli, F. O'Hara, C.,
824 Scarborough, C. and Selkoe, K. A., 2019. Recent pace of change in human impact on
825 the world's ocean. Scientific Reports, 9:11609. https://doi.org/10.1038/s41598-019-
826 47201-9.
827 Hayward, B.W.; Le Coze, F.; Vachard, D. and Gross, O. 2021. World Foraminifera Database.
828 Accessed at http://www.marinespecies.org/foraminifera on 2021-03-12.
829 https://doi.org/10.14284/305.

Heron-Allen, E. and Earland, A., 1914. The Foraminifera of the Kerimba Archipelago (Portuguese East Africa) - Part I. Transactions of the Zoological Society of London. 20(12): 363-390.

Hess, S., Jorissen, F.J., Venet, V. and Abu-Zied, R., 2005. Benthic foraminiferal recovery after recent turbidite deposition in Cap Breton canyon, Bay of Biscay. Journal of Foraminiferal Research, 35 (2), 114-129.

Hess, S. and Jorissen, F.J., 2009. Distribution patterns of living benthic foraminifera from Cap Breton canyon, Bay of Biscay: Faunal response to sediment instability. Deep-Sea Research Part I, 56 (9), 1555-1578.

Koho, K.A., Kouwenhoven, T.J., de Stigter, H.C. and van der Zwaan, G.J., 2007. Benthic foraminifera in the Nazaré Canyon, Portuguese continental margin: Sedimentary environments and disturbance. Marine Micropaleontology, 66 (1), 27-51.

Jones, R.W., 1994. The Challenger Foraminifera. Oxford Science Publications - The Natural History Museum, 149 pp.

Jorissen, F.J., Fontanier, C., Thomas, E. and Claude Hillaire-Marcel and de Vernal, A., 2007. Chapter Seven Paleoceanographical Proxies Based on Deep-Sea Benthic Foraminiferal Assemblage Characteristics, Developments in Marine Geology. Elsevier, pp. 263-325.

Labry, C., Herbland, A., Delmas, D., Laborde, P., Lazure, P., Froidefond, J. M., Jegou, A. M. and Sautour, B., 2001. Initiation of winter phytioplankton blooms within the Gironde plume waters in the Bay of Biscay. Marine Ecology Progress Series, 212, 117-130.

Lamarque, B., Deflandre, B., Galindo Dalto, A., Schmidt, S., Romero-Ramirez, A., Garabetian, F., Dubosq, N., Diaz, M., Grasso, F., Sottolichio, A., Bernard, G., Gillet, H., Cordier, M.-A., Poirier, D., Lebleu, P., Deriennic, H., Danilo, M., Murilo Barboza Tenório, M. and Grémare, A., 2021. Spatial distributions of surface sediment and

Sediment Profile Image characteristics in a high energy temperate marine RiOMar: the West Gironde Mud Patch. Journal of Marine Science and Engeneering, 9(3), 242 (32 p.). https://doi.org/10.3390/jmse9030242.

Lamarque, B., Deflandre, B., Schmidt, S., Bernard, G., Dubosq, N., Diaz, M., Lavesque, N., Garabetian, F., Grasso, F., Sottolichio, A., Rigaud, S., Romero-Ramirez, A., Cordier; M.-A., Poirier, D., Danilo, M. and Grémare, A., 2022. Spatiotemporal dynamics of surface sediment characteristics and benthic macrofauna compositions in a temperate high-energy River-dominated Ocean Margin. Continental Shelf Research, 247. https://doi.org/10.1016/j.csr.2022.104833

Lampert, L., Queguiner, B., Labasque, T., Pichon, A. and Lebreton, N., 2002. Spatial variability of phytoplankton composition and biomass on the eastern continental shelf of the Bay of Biscay (north-east Atlantic Ocean). Evidence for a bloom of *Emiliania huxleyi* (Prymnesiophyceae) in spring 1998. Continental Shelf Research, 22, 1225–1247.

Lampert, L., 2001. Dynamique saisonnière et variabilité pigmentaire des populations phytoplanctoniques dans l'atlantique nord (Golfe de Gascogne). Thèse d'Etat, Université de Bretagne Occidentale, 340 p.

Langezaal, A.M., Jorissen, F.J., Brauna, B., Chailloud, G., Fontanier, C., Anschutz, P. and van der Zwaan G.J. 2006. The influence of seasonal processes on geochemical profiles and foraminiferal assemblages on the outer shelf of the Bay of Biscay. Continental Shelf Research, 26(15), 1730-1755.

Langlet, D., Baal, C., Geslin, E., Metzger, E., Zuschin, M., Riedel, B., Risgaard-Petersen, N., Stachowitsch, M., and Jorissen, F. J., 2014. Foraminiferal species responses to in situ, experimentally induced anoxia in the Adriatic Sea, Biogeosciences, 11, 1775–1797, https://doi.org/10.5194/bg-11-1775-2014, 2014.

880 Lesueur, P., Tastet, J.P. and Marambat, L., 1996. Shelf mud fields formation within historical
881 times: examples from offshore the Gironde estuary, France. Continental Shelf
882 Research, 16, 1849–1870.
883 Lesueur, P., Tastet, J.P. and Weber, O., 2002. Origin and morphosedimentary evolution of
884 fine grained modern continental shelf deposits: the Gironde mud fields (Bay of
885 Biscay, France). Sedimentology, 49, 1299–1320.
886 Mamo, B. L., Cybulski, J. D., Hong, Y., Harnik, P.G., Chao, A., Tsujimoto, A., Wei, C. L.,
887 Baker, D. M. and Moriaki Yasuhara, M., 2023. Modern biogeography of benthic
888 foraminifera in an urbanized tropical marine ecosystem. Geological Society, London,
889 Special Publications 529 (1), SP529-2022-175, http://dx.doi.org/10.1144/sp529-2022-
890 175
891 Massé, C., Meisterhans, G., Deflandre, B., Bachelet, G., Bourasseau, L., Bichon, S., Ciutat,
892 A., Jude-Lemeilleur, F., Lavesque, N., Raymond, N., Grémare, A. and Garabetian, F.,
893 2016. Bacterial and macrofaunal communities in the sediments of the West Gironde
894 Mud Patch, Bay of Biscay (France). Estuarine, Coastal and Shelf Science, 179, 189-
895 200.
896 McKee, B.A., Aller, R.C., Allison, M.A., Bianchi, T.S. and Kineke, G.C., 2004. Transport
897 and transformation of dissolved and particulate materials on continental margins
898 influenced by major rivers: benthic boundary layer and seabed processes. Continental
899 Shelf Research, 24(7-8), 899-926.
900 Mendes, I., Dias, J. A., Schönfeld, J. and Ferreira, Ó., 2012. Distribution of living benthic
901 foraminifera on the northern Gulf of Cadiz continental shelf. Journal of Foraminiferal
902 Research, 42, 18–38
903 Migeon, S., Weber, O., Faugères, J.-C. and Saint-Paul, J., 1999. SCOPIX: a new X-ray
904 imaging system for core analysis. Geo-Marine Letters, 18, 251-255.

905 Murray, J.W., 2006. Ecology and Applications of Benthic Foraminifera. Cambridge
906 University Press, pp 426.
907 Murray, J.W. and Bowser, S.S., 2000. Mortality, protoplasm decay rate, and reliability of
908 staining techniques to recognize 'living' foraminifera: a review. Journal of
909 Foraminiferal Research, 30, 66-70.
910 Natsir, S. M.., 2022. The distribution of benthic foraminifera in coral reefs ecosystem of East
911 Penjaliran Island, Seribu Islands, Indonesia. Biodiversitas Journal of Biological
912 Diversity, 23(6), ttps://doi.org/10.13057/biodiv/d230634.
913 Orbigny, A. D. d'., 1826. Tableau méthodique de la classe des Céphalopodes. Annales des
914 Sciences Naturelles, vol. 7: 96-169, 245-314.
915 Orbigny, A. D. d'., 1839. Foraminifères des îles Canaries. Histoire naturelle des Iles Canaries.
916 2(2): 120-146.
917 Schönfeld, J., Alve, E., Geslin, E., Jorissen, F., Korsun, S., Spezzaferri, S., Abramovich, S.,
918 Almogi-Labin, A., du Chatelet, E.A., Barras, C., Bergamin, L., Bicchi, E., Bouchet,
919 V., Cearreta, A., Di Bella, L., Dijkstra, N., Disaro, S.T., Ferraro, L., Frontalini, F.,
920 Gennari, G., Golikova, E., Haynert, K., Hess, S., Husum, K., Martins, V., McGann,
921 M., Oron, S., Romano, E., Sousa, S.M. and Tsujimoto, A., 2012. The FOBIMO
922 (FOraminiferal BIo-MOnitoring) initiative-Towards a standardised protocol for soft
923 bottom benthic foraminiferal monitoring studies. Marine Micropaleontology, 94–95,
924 1–13. https://doi.org/10.1016/j.marmicro.2012.06.001.
925 Stevenson, F.J. and Cheng, C.N., 1970. Amino acids in sediments: Recovery by acid
926 hydrolysis and quantitative estimation by a colorimetric procedure. Geochimica et
927 Cosmochimica Acta, 34, 77-88.
928 Toyofuku, T., Duros, P., Fontanier, C., Mamo, B., Bichon, S., Buscail , R., Chabaud, G.,
929 Deflandre, B., Goubet, S., Grémare, A., Menniti, C., Fujii, M., Kawamura, K. Koho,

930 K.A., Noda, A., Namegaya, Y., Oguri, K., Radakovitch, O., Murayama, M., De
931 Nooijer, L.J., Kurasawa, A., Ohkawara, N., Okutani, T., Sakaguchi, A., Jorissen, F.,
932 Reichart, G.J. and Kitazato, H., 2014. Unexpected biotic resilience on the Japanese
933 seafloor caused by the 2011 Tôhoku-Oki tsunami. Scientific Reports, 4, 7517.
934 Tsujimoto, A., Nomura, R., Arai, K., Nomaki, H., Inoue, M. and Fujikura, K., 2020. Changes
935 in deep-sea benthic foraminiferal fauna caused by turbidites deposited after the 2011
936 Tohoku-oki earthquake. Marine Geology, 419, 106045 https://doi.org/10.1016/j.
937 Walton, W.R., 1952. Techniques for recognition of living Foraminifera. Contributions from
938 the Cushman Foundation for Foraminiferal Research, 3, 56-60.
939

Appendix captions

Appendix A

Major foraminiferal species (≥ 5%) identified in the West-Gironde Mud Patch, with reference to plates and figures in the literature. Supplementary data associated with this article can be consulted in the online version at xxxx.

Appendix B

Census data for live (stained) benthic foraminifera in the >150 µm fraction for the three stations sampled in the West-Gironde Mud Patch and for the three sampling periods. N.B. Numbers are not standardized for sediment volume. Supplementary data associated with this article can be consulted in the online version at xxxx.